The Marconi Review

No. 126 3rd QUARTER 1957 Vol. XX

CONTENTS:

MARCONI'S WIRELESS TELEGRAPH COMPANY LIMITED

Head Office, Marconi House, Chelmsford Telephone, Chelmsford 3221 Telegraphic Address, Expanse, Chelmsford

THE MARCONI GROUP OF COMPANIES IN GREAT BRITAIN

Registered Office: Marconi House,
Strand,
London, W.C.2.

Telephone: Covent Garden 1234.

MARCONI'S WIRELESS TELEGRAPH COMPANY, LIMITED

Marconi House,
Chelmsford,
Essex.

Telephone: Chelmsford 3221.
Telegrams: Expanse, Chelmsford.

THE MARCONI INTERNATIONAL MARINE COMMUNICATION COMPANY, LIMITED

Marconi House,
Chelmsford,
Essex.

Telephone: Chelmsford 3221.
Telegrams: Thulium, Chelmsford.

THE MARCONI SOUNDING DEVICE COMPANY, LIMITED

Marconi House,
Chelmsford,
Essex.

Telephone: Chelmsford 3221.
Telegrams: Thulium, Chelmsford.

THE RADIO COMMUNICATION COMPANY, LIMITED

Marconi House,
Chelmsford,
Essex.

Telephone: Chelmsford 3221.
Telegrams: Thulium, Chelmsford.

THE MARCONI INTERNATIONAL CODE COMPANY, LIMITED

Marconi House,
Strand,
London, W.C.2.

Telephone: Covent Garden 1234.
Telegrams: Docinocram.

MARCONI INSTRUMENTS, LIMITED

St. Albans,
Hertfordshire.

Telephone: St. Albans 6161/5.
Telegrams: Measurtest, St. Albans.

SCANNERS LIMITED

Woodskinners Yard,
Bill Quay,
Gateshead, 10,
Co. Durham.

Telephone: Felling 82178.
Telegrams: Scanners, Newcastle-upon-Tyne.

THE MARCONI REVIEW

No. 126 Vol. XX *3rd Quarter, 1957*

Editor : L. E. Q. WALKER, A.R.C.S.

PROPAGATION AND THE RADIO ART

TO many engineers radio implies the development of apparatus and the design of new circuits. The radio art does not, however, consist only in the building of transmitters and receivers. Fundamentally it rests on the propagation of electromagnetic waves first realized by Maxwell as a possibility from a set of mathematical equations and shown by Hertz twenty-five years later to be a practical reality.

The advancement of the art has depended vitally on propagation research with its intimate interplay of theory and experiment. Marconi's name is for all time associated with the brilliant exploitation of the experimental method in the face of general scientific opinion, while the successful commercial use of waves propagated round the earth has been greatly advanced by the knowledge gained from the magneto-ionic theory of wave propagation in the ionosphere in the presence of the earth's magnetic field.

In the opening up in turn of further parts of the radio spectrum, the development of new techniques and propagation research have gone hand in hand in making possible the various uses to which radio has been put. Hertz conducted his original experiments in what is now called the ultra high frequency band, and it has been the introduction of advanced types of valves and highly stable oscillators, together with waveguide techniques and high gain aerial systems, that has brought about the amazing progress that has been made in this field.

Even so, the characteristics of the propagation medium have determined many of the techniques needed in the successful use of radio in all parts of the spectrum. Both the ionosphere and the troposphere have a complicated structure varying from place to place and subject to great variations with time, not only from moment to moment, but diurnally, seasonally and even from year to year. The surface of the earth itself has many irregularities making the use of ground-wave propagation for

television broadcasting and relay links far less straightforward than it would otherwise be.

It would make an interesting study to trace the origin of the many features of transmitter and receiver design, so often taken for granted by the engineer who has to incorporate them in his apparatus, that have been introduced to combat ill effects of phenomena that are the result of the vagaries of the propagation medium and Nature's own array of radio transmitters. What efforts have been put into overcoming terrestrial noise in its many forms, quite apart from the interference caused by man-made noise, unwanted harmonics and the like. What problems have arisen from multipath transmission in all its forms and from fading troubles in all parts of the radio spectrum. What difficulties have been met due to the congested state of the spectrum and in the use of common frequencies under conditions in which it was hoped they would not mutually interfere.

In the use of radio for direction-finding, radar and navigational aids one has only to mention such terms as " night effect, polarization error, coastal refraction, back scattering, Doppler effects, anomalous propagation, etc.", to realize how profoundly the behaviour of the propagation medium in its broadest sense controls the work of the engineer. The new methods of communication for forward-scattering in the ionosphere and troposphere using very high effective radiated powers have yet to be the subject of much propagation research before the circumstances of their full exploitation are known and the difficulties imposed by the medium are overcome.

In the progress of radio Nature has given man the possibility of using electromagnetic waves over a wide range of frequencies for many purposes, but with each new application she has striven, seemingly, to prevent the perfect attainment of his objective. He has replied by devising new techniques to overcome the difficulties placed in his way. The use of various forms of diversity transmission and reception, single sideband working, frequency modulation, error correcting codes, frequency shift keying and spaced frame direction finders are but some of the techniques which are associated in one way or another with this contest to achieve man's ends.

Ultimately Nature may have the last word and may set the final limit, but the challenge that she presents still continues to stimulate the ingenuity of man in surmounting the barriers to further progress. Propagation research seeks to discover the new roads of advance and to point out the pitfalls along the way. In this adventure there is needed the co-operation of the engineer who finds the way round the difficult places and brings the project to fruition in some new application for the use of mankind.

G. Millington.

THE CONCEPT OF THE EQUIVALENT RADIUS OF THE EARTH IN TROPOSPHERIC PROPAGATION

By G. Millington, M.A., B.Sc., M.I.E.E.

The concept of the equivalent radius of the earth to take account of a linear variation of refractive index with height in tropospheric refraction is re-examined. It is shown that the transformation is not limited to nearly horizontal rays, but that essentially it reduces the curvature of the earth by that of a ray travelling horizontally and the curvature of the rays by the amount required to straighten them at whatever angle to the horizontal they may be going. The results obtained geometrically in a previous paper for the angle of elevation at the reflection point, the optical path difference between the direct and indirect rays and the divergence factor are derived by simple analysis, affording a useful check on the method.

Introduction

In an earlier paper(1), here referred to as I, the author has considered the modification to the results for a flat earth produced by the curvature of the earth in the geometric-optical treatment of ground-wave propagation within the horizon. Many equivalent solutions of this problem have been given, some of which are referred to in the books edited by Burrows and Attwood(2) and by Kerr(3).

In this problem it is usual to take into account the effect of the troposphere by assuming that its refractive index decreases linearly with height above the ground and then applying a transformation that straightens the rays and reduces the curvature of the earth accordingly. Schelleng, Burrows and Ferrell(4) examined the nature of this transformation by using a model for the troposphere for which the ray equation could be solved in exact form and showed that the error involved was negligible provided that the ray paths were nearly horizontal.

It is the purpose of the present paper to examine this matter from first principles and to show more clearly the approximations upon which the transformation is based. The results will be developed in the form used in I to show that the method there given of using the equivalent radius of the earth was correct.

Radius of Curvature of the Ray Paths

It is convenient here to give a simple derivation of the well-known expression for the curvature of the ray paths in terms of the gradient of refractive index. In Fig. 1 an element of phase surface FG moves along the ray path into the position F′G′. If the phase velocity along the arc FF′ is v and that along GG′ is $v + \delta v$, then

$$\frac{\delta v}{v} = \frac{\delta R}{R} \tag{1}$$

where R is the radius of curvature of the arc FF′.

In terms of the refractive index μ, the phase velocity is given by

$$v = \frac{c}{\mu}$$

where c is the free space velocity, so that

$$\frac{\delta v}{v} = -\frac{\delta \mu}{\mu} \tag{2}$$

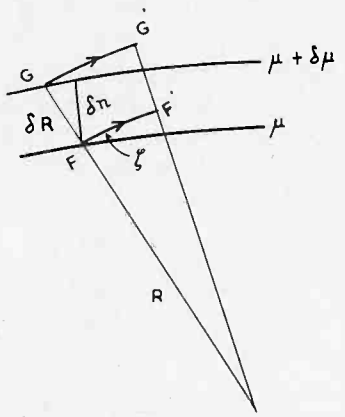

FIG. 1

Thus from equations (1) and (2)

$$\frac{1}{R} = -\frac{1}{\mu}\frac{\delta \mu}{\delta R} \tag{3}$$

If, as in Fig. 1, the ray path makes an angle ζ with the surface of constant refractive index, then with reference to the Figure,

$$\delta n = \delta R \cos \zeta \tag{4}$$

and thus from equations (3) and (4)

$$\frac{1}{R} = -\frac{1}{\mu}\frac{\partial \mu}{\partial n}\cos \zeta \tag{5}$$

where $\frac{\partial \mu}{\partial n}$ is the gradient of refractive index at the point under consideration.

The Ray Path in the Troposphere

In applying the above results to the troposphere, it is assumed that the surfaces of constant refractive index are spheres concentric with the earth, so that the gradient $\frac{\partial \mu}{\partial n}$ is equal to $\frac{d\mu}{dh}$ where h is height above the ground. Furthermore this gradient is assumed to be constant, so that the refractive index as a function of height is

$$\mu = \mu_0 + \frac{d\mu}{dh} \cdot h \tag{6}$$

where μ_0 is the value at the ground.

Actually μ_0 could be taken as unity since it exceeds it by only about 3×10^{-4}, but it will be formally retained for the sake of completeness and because it stresses the importance of the gradient of refractive index even when the overall changes are small.

With this model, equation (5) becomes

$$\frac{1}{R} = -\frac{1}{\mu}\frac{d\mu}{dh}\cos \zeta \tag{7}$$

and if R_0 is the radius of curvature of a ray travelling horizontally immediately above the surface of the earth

$$\frac{1}{R_0} = -\frac{1}{\mu_0}\frac{d\mu}{dh} \tag{8}$$

so that equation (6) may be written

$$\mu = \mu_0 \left[1 - \frac{h}{R_0}\right] \tag{9}$$

Suppose now that in Fig. 2, PQ is an element of length δp of a ray path extending from A to B and that it subtends an angle $\delta\psi$ at the centre of curvature of the ray path at P. If the corresponding element PM along the horizontal arc through P subtends an angle $\delta\varphi$ at the centre of the earth, then since $\angle QPM = \zeta$,

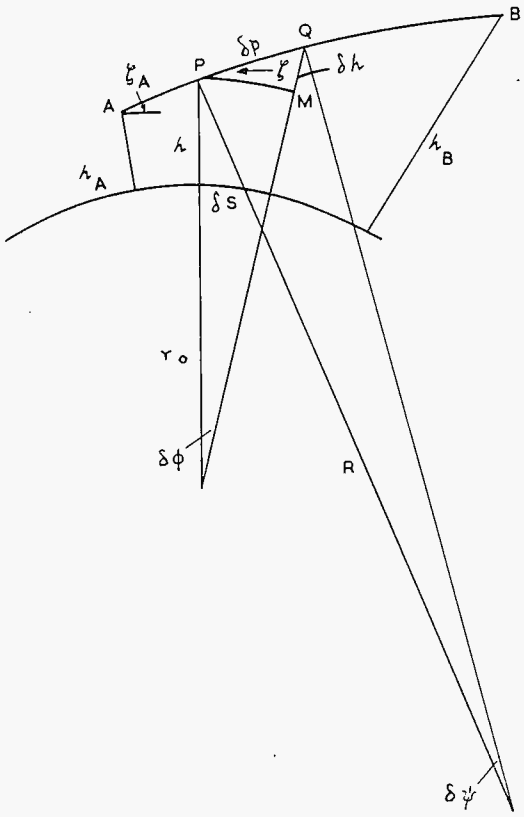

FIG. 2

$$\cos\zeta = \frac{PM}{PQ} = \frac{(r_0 + h)\,\delta\varphi}{R\delta\psi}$$

which when substituted in equation (7) gives

$$\delta\psi = \left[-\frac{1}{\mu}\frac{d\mu}{dh}\right](r_0 + h)\,\delta\varphi$$

i.e., from equation (8)

$$\delta\psi = \frac{\mu_0}{\mu}\frac{(r_0 + h)}{R_0}\,\delta\varphi \tag{10}$$

If δs is the corresponding distance measured over the curved surface of the earth

$$\delta s = r_0\,\delta\varphi \tag{11}$$

and equation (10) may be written

$$\delta\psi = \frac{\mu_0}{\mu}\left(1 + \frac{h}{r_0}\right)\frac{\delta s}{R_0} \tag{12}$$

If the value of ζ at the starting point is ζ_A, then as the tangent to the ray path rotates in space through an angle ψ on passing from A to P while the horizontal direction rotates through an angle φ, it follows that

$$\zeta = \zeta_A + \varphi - \psi \tag{13}$$

Also as $MQ = \delta h$,

$$\delta h = (r_0 + h)\tan\zeta\,.\delta\varphi$$

i.e., from equation (11)

$$\delta h = \left(1 + \frac{h}{r_0}\right)\tan\zeta\,\delta s \tag{14}$$

while similarly

$$\delta p = \left(1 + \frac{h}{r_0}\right)\sec\zeta\,\delta s \tag{15}$$

These equations are subject to the initial conditions that $h = h_A$ and $\zeta = \zeta_A$ at $s = 0$.

From equations (9), (11), (12) and (13) it follows that

$$\delta\zeta = \left[\frac{1}{r_0} - \frac{1}{R_0} - \frac{2h}{r_0 R_0}\right] \frac{\delta s}{\left(1 - \frac{h}{R_0}\right)} \tag{16}$$

Equations (14) and (16) can be regarded as giving h as a function of s for the given initial conditions. Alternatively they give ζ_A as a function of h_A and h_B for a ray path which starts at a height h_A at $s = 0$ and ends at a height h_B at a distance $s = s_0$, say, measured over the surface of the earth.

The Equivalent Radius of the Earth

The form of equation (16) suggests the definition of an equivalent radius r_e given by

$$\frac{1}{r_e} = \frac{1}{r_0} - \frac{1}{R_0} \tag{17}$$

It is usually assumed that $R_0 = 4r_0$, so that $r_e = \frac{4}{3} r_0$, under normal or standard tropospheric conditions. In this introduction of the equivalent radius of the earth no limitation has been placed on the value of ζ_A which has not so far been restricted to small values corresponding to nearly horizontal rays.

The validity of the concept of the equivalent radius depends upon being able to express the solution of the ray path equations to a sufficient degree of accuracy by that for a homogeneous atmosphere with r_0 everywhere replaced by r_e. It then becomes possible to solve the problem by using a geometrical transformation in which the earth has an equivalent radius r_e and the ray paths are straight.

In order to see under what restrictions, if any, this becomes possible, the equations will be considered first in rather general terms. The method to be adopted will be to assume that h can be expanded in a power series in s, and a preliminary consideration of the limiting conditions at low and high angles of elevation suggests that it is sufficient to limit the series to a quadratic form, so that

$$h = h_A + a\,s + b\,s^2 \tag{18}$$

where the coefficients a and b are determined by substituting equation (18) in equations (14) and (16), thereby giving equation (18) as the equation of the ray path.

Height and Angle Relationships

The integral form of equation (14) is

$$\int_{h_A}^{h} dh = \int_0^s \left(1 + \frac{h}{r_0}\right) \tan\zeta \, ds$$

so that from equation (18)

$$a\,s + b\,s^2 = \int_0^s \left(1 + \frac{h}{r_0}\right) \tan\zeta \, ds \tag{19}$$

Thus in order to determine a and b, it is necessary to expand the integrand in equation (19) only to the first power in s. The value of ζ is given from equations (16) and (17) by

$$\int_{\zeta_A}^{\zeta} d\zeta = \int_0^s \left[\frac{1}{r_e} - \frac{2h}{r_0 R_0}\right] \frac{ds}{\left(1 - \frac{h}{R_0}\right)} \tag{20}$$

For use in equation (19), the integrand on the right hand side of equation (20) needs only to be expanded as far as the constant term, so that from equation (18), equation (20) gives

$$\zeta = \zeta_A + c\,s \tag{21}$$

where

$$c = \left[\frac{1}{r_e} - \frac{2h_A}{r_0 R_0}\right] \Big/ \left[1 - \frac{h_A}{R_0}\right] \tag{22}$$

By taking the first two terms of a Taylor expansion, equation (21) gives

$$\tan\zeta = \tan\zeta_A + c\,s\,\sec^2\zeta_A \tag{23}$$

Thus from equations (18) and (23), to the first power in s

$$\left(1 + \frac{h}{r_0}\right)\tan\zeta = \left(1 + \frac{h_A}{r_0}\right)\tan\zeta_A + \left[\frac{a}{r_0}\tan\zeta_A + \left(1 + \frac{h_A}{r_0}\right) c\,\sec^2\zeta_A\right] s$$

so that on integration of equation (19)

$$a = \left(1 + \frac{h_A}{r_0}\right)\tan\zeta_A \tag{24}$$

and

$$b = \frac{1}{2}\left[\frac{a}{r_0}\tan\zeta_A + \left(1 + \frac{h_A}{r_0}\right) c\,\sec^2\zeta_A\right]$$

i.e., from equation (24)

$$b = \frac{1}{2}\left(1 + \frac{h_A}{r_0}\right)\left[\frac{1}{r_0}\tan^2\zeta_A + c\,\sec^2\zeta_A\right] \tag{25}$$

In order to establish the equivalence theorem, it is now necessary to invoke the condition that the heights considered in tropospheric propagation are very small compared with the radius of the earth, so that equation (22) gives

$$c = \frac{1}{r_e} \tag{26}$$

and equations (24) and (25) become

$$a = \tan\zeta_A \tag{27}$$

$$b = \frac{1}{2}\left[\frac{1}{r_e} + \left(\frac{1}{r_0} + \frac{1}{r_e}\right)\tan^2\zeta_A\right] \tag{28}$$

Thus from equations (18), (27) and (28)

$$h = h_A + s\tan\zeta_A + \frac{s^2}{2r_e}\left[1 + \left(1 + \frac{r_e}{r_0}\right)\tan^2\zeta_A\right] \tag{29}$$

At first sight it appears that for large values of $\tan \zeta_A$ the power series for h diverges, but for a given value of $h - h_A$, s decreases as $\tan \zeta_A$ increases and their product approaches the flat earth limit of $h - h_A$. On the other hand when $\tan \zeta_A$ is sufficiently small, $s \tan \zeta_A$ becomes small compared with $s^2/2r_e$.

If
$$s \tan \zeta_A = (h - h_A)(1 - \alpha) \tag{30}$$

and
$$\frac{s^2}{2r_e} = (h - h_A)(1 - \beta) \tag{31}$$

then as $\zeta_A \to 0$, $\alpha \to 1$ and $\beta \to 0$

and as $\zeta_A \to \frac{\pi}{2}$, $\alpha \to 0$ and $\beta \to 1$.

On substituting equations (30) and (31) in equation (29) and dividing through by $h - h_A$, it will be found that
$$\alpha + \beta = 1 + \frac{h - h_A}{2r_e}\left(1 + \frac{r_e}{r_0}\right)(1 - \alpha)^2 \tag{32}$$

Now from equations (30) and (31)
$$s \tan \zeta_A + \frac{s^2}{2r_e} = (h - h_A)(2 - \alpha - \beta)$$

i.e., from equation (32)
$$s \tan \zeta_A + \frac{s^2}{2r_e} = (h - h_A)\left[1 - O\left(\frac{h - h_A}{r_e}\right)\right]$$

Thus over the whole range of ζ_A equation (29) may be replaced to the order of accuracy under consideration by
$$h = h_A + s \tan \zeta_A + \frac{s^2}{2r_e} \tag{33}$$

in which the s^2 term is of course already negligible under conditions in which $\tan^2 \zeta_A$ is not $<< 1$.

The fact that $s \tan \zeta_A$ approaches the limit $h - h_A$ as $\zeta_A \to \frac{\pi}{2}$ assures the convergence of the power series for h and justifies the restriction to the quadratic form in equation (18).

It follows from equation (33) that for $h = h_B$ and $s = s_0$
$$\tan \zeta_A = \frac{h_B - h_A}{s_0} - \frac{s_0}{r_e} \tag{34}$$

In equations (33) and (34), r_0 does not appear explicitly, and if the case for a homogeneous atmosphere is derived by putting $R_0 = \infty$, r_e in these equations is replaced by r_0. It follows that they have the same form that they would have for a homogeneous atmosphere above an earth of radius r_e, and the equivalence theorem is established as far as the height and angle relationship is concerned.

Using the geometrical transformation in which the ray paths are straight and the earth has an equivalent radius r_e, equation (34) may be derived by simple

geometry along the lines of the proof given in I. It is interesting to note that for the case when $h_A = 0$, i.e., for a ray starting at the surface of the earth where ζ_A is equal, say, to θ, the geometrical proof leads formally to the expansion

$$h = s \tan \theta + \frac{s^2}{2r_e}\left[1 + 2 \tan^2 \theta\right] \tag{35}$$

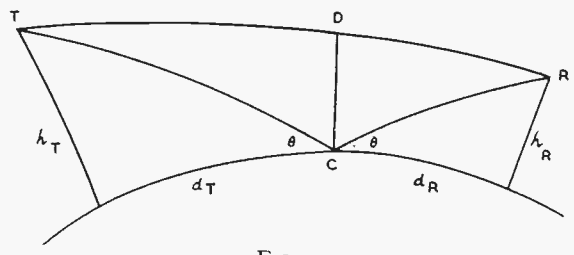

FIG. 3

which confirms the general form of equation (29), though it does not of course affect the validity of the approximation in equation (33) upon which the equivalence theorem is based.

Consider now the ray paths shown in Fig. 3 between a transmitter T at a height h_T and a receiver R at a height h_R and a distance d away measured over the surface of the earth. Let the reflection point for the indirect ray be C which divides d into the parts d_T and d_R for the ray paths TC and CR so that

$$d = d_T + d_R \tag{36}$$

Suppose that the angle of elevation at C is θ, which by the law of reflection is the same for both paths, regarding the path TC in the reverse sense from C to T for convenience.

Equation (34) may be applied to the path CT by putting $\zeta_A = \theta$, $h_A = 0$, $h_B = h_T$ and $s_0 = d_T$, so that

$$\tan \theta = \frac{h_T}{d_T} - \frac{d_T}{2r_e} \tag{37}$$

and similarly for the path CR

$$\tan \theta = \frac{h_R}{d_R} - \frac{d_R}{2r_e} \tag{38}$$

By using equation (36), equations (37) and (38) may be solved for d_T (or d_R) and tan θ, giving the angle of elevation and the position of the reflection point. The cubic equation obtained in the process may be solved graphically exactly as in I using the charts there given.

In the transformed picture the same actual heights and distance d apart of the transmitter and receiver are used, and the position of the reflection point and the value of the angle of elevation are the same as in the actual situation in Fig. 3. This is of practical importance where in reality ground irregularities may exist and it is necessary to see whether the reflection point given by the idealized smooth earth picture is affected by any irregularities in the region.

The Path Difference Formula

The phase difference between the signals at R arriving by the direct path TR in Fig. 3 and by reflection at C depends upon the difference of the corresponding optical paths. For small values of elevation this difference is very small compared

with the length of the individual paths and it is not legitimate to neglect small terms in the integrals without careful consideration.

The optical path p' is given by

$$p' = \int \mu \, d \, p \tag{39}$$

taken between appropriate limits.

From equations (9) and (15), equation (39) may be written

$$p' = \int_0^s \mu_0 \left(1 - \frac{h}{R_0}\right) \left(1 + \frac{h}{r_0}\right) \sec \zeta \, d \, s \tag{40}$$

An attempt to expand the integrand as a power series in s as far as the s^2 term, so that p' is given to the s^3 term required for the differencing process, is laborious. The essential condition is now to retain terms in the integrand of order $\frac{h}{r_0}$ while neglecting the extremely small terms of order $\frac{h^2}{{r_0}^2}$. Thus it is permissible with the use of equation (17) to write

$$\left(1 - \frac{h}{R_0}\right) \left(1 + \frac{h}{r_0}\right) = 1 + \frac{h}{r_e} \tag{41}$$

In this equation h can be replaced by its value in equation (33), since the approximations made in deriving it from equation (14) correspond to the neglect of terms of order $\frac{h^2}{{r_0}^2}$ in equation (41).

Returning to equation (20), by the mean value theorem it may be written

$$\int_{\zeta_A}^{\zeta} d \, \zeta = \int_0^s \frac{1}{r_e} (1 - \gamma) \, d \, s$$

where γ is a constant of the order of h/R_0, so that

$$\zeta = \zeta_A + \frac{1}{r_e} (1 - \gamma) \, s$$

The Taylor expansion for $\sec \zeta$ as far as the s^2 term is thus given by

$$\sec \zeta = \sec \zeta_A + \sec \zeta_A \tan \zeta_A \frac{(1 - \gamma)}{r_e} s + \sec \zeta_A \, (1 + 2 \tan^2 \zeta_A) \frac{(1 - \gamma)^2}{2 {r_e}^2} s^2$$

By an argument similar to that used above, remembering that γ is of the order of h/R_0, the neglect of terms of order $h^2/{r_0}^2$ leads to

$$\sec \zeta = \sec \zeta_A \left[1 + \frac{s}{r_e} \tan \zeta_A + \frac{s^2}{2 {r_e}^2}\right]$$

which from equation (33) may be put in the form

$$\sec \zeta = \sec \zeta_A \left[1 + \frac{h - h_A}{r_e}\right]$$

With equation (41) this gives

$$\left(1 - \frac{h}{R_0}\right)\left(1 + \frac{h}{r_0}\right) \sec \zeta = \sec \zeta_A \left[1 + \frac{2h - h_A}{r_e}\right]$$

so that equation (40) becomes

$$p' = \mu_0 \sec \zeta_A \int_0^s \left[1 + \frac{2h - h_A}{r_e}\right] d\,s \tag{42}$$

where h is given by equation (33) and ζ_A by equation (34).

In view of the equivalence theorem already established for h and ζ_A, it follows from equation (42) that the equivalence also holds for the optical path difference, replacing the atmosphere by one which is homogeneous with a refractive index μ_0 and the earth by a sphere of radius r_e, without any formal restriction to small values of ζ_A.

However, at high angles of elevation the path difference between the direct and indirect rays is no longer very small compared with the lengths of the individual paths, since the distance along the ground between the transmitter and receiver is then only comparable with their heights above the surface. Moreover, the ground irregularities make a precise calculation of the path difference at large angles of elevation based on an ideal theory unwarranted, especially where the terminal heights are large compared with the wavelength and the path difference may contain many wavelengths. It is only at small angles of elevation in the study of the interference pattern near the horizon that the problem is of practical importance.

In any case the direct integration of equation (42) using equations (33) and (34) would lead to a cumbersome result and it would be simpler to resort to a geometrical solution based on the equivalence theorem. However, it is interesting as a check on the analytical approach adopted here to derive the form of the result given in I for small angles of elevation.

In equation (42), h is given its value in equation (33) with tan ζ_A put equal to ζ_A, and sec ζ_A is replaced by $1 + \zeta_A^2/2$, so that

$$p' = \mu_0 \int_0^s \left(1 + \frac{\zeta_A^2}{2}\right)\left(1 + \frac{h_A}{r_e} + \frac{2\zeta_A s}{r_e} + \frac{s^2}{r_e^2}\right) d\,s$$

which can be written for the small values of ζ_A under consideration as

$$p' = \mu_0 \int_0^s \left(1 + \frac{h_A}{r_e} + \frac{s^2}{r_e^2} + \frac{\zeta_A^2}{2} + \frac{2\zeta_A s}{r_e}\right) d\,s \tag{43}$$

This result can be obtained more simply by approximating directly to sec ζ in equation (40) by $1 + \zeta^2/2$, where ζ is given from equations (21) and (26) by $\zeta_A + \frac{s}{r_e}$, and again using equations (41) and (33).

Referring back to Fig. 3 it is useful to divide the path TR into two parts TD and DR, where D is at a distance d_T from T measured over the surface of the earth. The optical path difference corresponding to the path TC + CR − TR may then be split up into TC − TD and RC − RD. For TC and TD the upper limit in both cases for the integral in equation (43) is d_T, and it leads to a considerable simplification to do part of the differencing in the integrands before integration. For both paths

the starting point is T, so that h_A is the same for both, namely h_T. Thus in equation (43), $1 + \frac{h_A}{r_e} + \frac{s^2}{r_e^2}$ is common to both integrands, so that it is only necessary to consider the difference between integrals of the form

$$I = \mu_0 \int_0^{d_T} \left[\frac{\zeta_A^2}{2} + \frac{2\zeta_A s}{r_e}\right] ds = \mu_0 \frac{d_T}{2}\left[\zeta_A^2 + 2\zeta_A \frac{d_T}{r_e}\right] \tag{44}$$

Now in considering the path TC in the opposite direction, it has been seen that at C, $\zeta_A = \theta$, and thus from equations (21) and (26) $\zeta = \theta + \frac{d_T}{r_e}$ at T. It follows that in the direction TC,

$\zeta_A = -\left(\theta + \frac{d_T}{r_e}\right)$ at T, and so from equation (44) on reduction

$$I_{TC} = \mu_0 \frac{d_T}{2}\left[\theta^2 - \frac{d_T^2}{r_e^2}\right] \tag{45}$$

Suppose for the moment that, for the path TD, the value of ζ_A at T is ζ_T, then from equation (44)

$$I_{TD} = \mu_0 \frac{d_T}{2}\left[\zeta_T^2 + 2\zeta_T \frac{d_T}{r_e}\right] \tag{46}$$

The required optical path difference for TC — TD is from equations (45) and (46) given by

$$I_{TC} - I_{TD} = \mu_0 \frac{d_T}{2}\left[\theta^2 - \left(\zeta_T + \frac{d_T}{r_e}\right)^2\right] \tag{47}$$

The value of ζ_T may be found from equation (34) for the path TR by putting $\tan \zeta_A = \zeta_T$, $h_A = h_T$, $h_B = h_R$ and $s_0 = d$, so that

$$\zeta_T = \frac{h_R - h_T}{d} - \frac{d}{2r_e} \tag{48}$$

where d is the total distance between T and R, as in equation (36).

Now from equations (37) and (38) for small values of θ

$$h_T = d_T\,\theta + \frac{d_T^2}{2r_e} \tag{49}$$

and

$$h_R = d_R\,\theta + \frac{d_R^2}{2r_e} \tag{50}$$

Thus from equations (48), (49), (50) and (36) on reduction

$$\zeta_T = \frac{\theta\,(d_R - d_T)}{d} - \frac{d_T}{r_e}$$

and hence

$$\zeta_T + \frac{d_T}{r_e} = \frac{\theta\,(d_R - d_T)}{d} \tag{51}$$

It follows from equations (36) and (51) that

$$\theta^2 - \left(\zeta_T + \frac{d_T}{r_e}\right)^2 = 4\frac{d_T\, d_R}{d^2}\,\theta^2 \tag{52}$$

and hence from equations (47) and (52) that

$$I_{TC} - I_{TD} = 2\mu_0 \frac{d_T^2\, d_R}{d^2}\,\theta^2 \tag{53}$$

The corresponding value for the path difference RC — RD can be obtained immediately from equation (53) by interchanging d_T and d_R, giving

$$I_{RC} - I_{RD} = 2\mu_0 \frac{d_R^2\, d_T}{d^2}\,\theta^2 \tag{54}$$

Finally by adding together equations (53) and (54), the optical path difference, say $\Delta p'$, is given by

$$\Delta p' = 2\mu_0 \frac{d_T\, d_R}{d}\,\theta^2 \tag{55}$$

This value agrees with that given in I, where μ_0 was taken as unity, and leads to a similar technique for expressing $\Delta p'$ as the flat-earth value multiplied by a factor that can be found from the graphs in I.

A point of some interest arises by returning to equation (40) and resolving it as follows:—

$$p' = \mu_0 [A - B] \tag{56}$$

where

$$A = \int_0^s \left(1 + \frac{h}{r_0}\right) \sec\zeta\, d\,s \tag{57}$$

and

$$B = \int_0^s \frac{h}{R_0}\left(1 + \frac{h}{r_0}\right) \sec\zeta\, d\,s \tag{58}$$

From equations (15) and (57) it follows that

$$A = p \tag{59}$$

while

$$B = \int_0^s \frac{h}{R_0}\, d\,s \tag{60}$$

where in equation (59) p is the actual geometrical path length, while in equation (60) the higher order terms in equation (58) are rejected.

Now A is very much greater than B, and as it takes account of the fact that the ray path is not straight but is a circular arc, it might be thought at first sight that it contains the significant part of the correction for the gradient of refractive index. It turns out, however, that although the individual paths given by B in equation (60) are very small, the relevant path difference contributed by B is comparable with that derived from A.

In fact, by a geometrical argument based on the assumption that the paths are circular arcs of radius R_0, it can be shown that the difference between the A terms is ΔA where

$$\Delta A = \frac{2d_T\, d_R}{d}\,\theta\left(\theta - \frac{\psi}{2}\right) \tag{61}$$

where ψ is the angle subtended by the arc TR at its centre of curvature.

From the integration of equation (60), using the value of h in equation (33) for small ζ_A, it can be shown that the corresponding value of ΔB is

$$\Delta B = -\frac{d_T\, d_R}{d}\,\theta\,\psi \tag{62}$$

which with equation (61) leads from equation (56) to equation (55).

Equation (61) shows that on the horizon, where $\theta = 0$, the geometrical path difference is zero, as is obvious, but that as θ is increased from zero, the path difference becomes negative and remains so until $\theta = \psi/2$. This means that there is an initial range of values for which the actual curved path for the direct ray is longer than the sum of the two components of the indirect ray path.

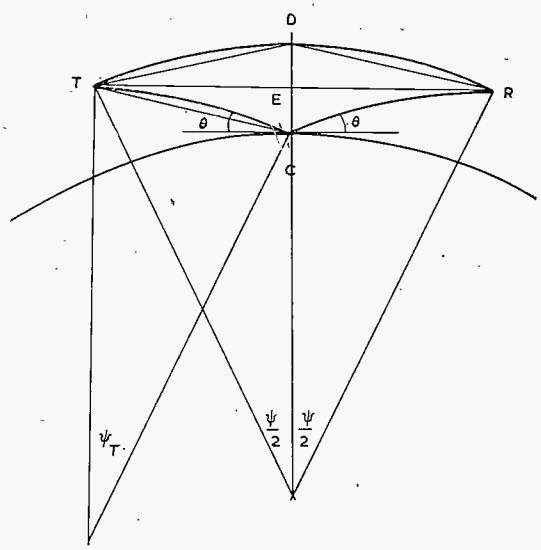

FIG. 4

The limiting case for $\theta = \psi/2$ is shown in Fig. 4 for the symmetrical situation in which $h_T = h_R$ and the line CD is bisected by the chord TR at E. It is obvious that the chord TD is equal to the chord TC, and as the arcs have the same radius R_0, they must also be equal. Thus the total arc TR is equal to the sum of the arcs TC and CR, so that the path difference is zero. The chord CT makes an angle $\theta - \psi_T/2$ with the tangent plane through C, where ψ_T is the angle subtended by the arc TC at its centre of curvature. This angle is equal to $\angle ETC = \angle DTE$. As $\psi_T = \psi/2$, it follows that $\angle DTE = \theta - \psi/4$, but this angle is half of the angle $\psi/2$ subtended by DR at the centre of curvature of the arc TDR, so that $\theta - \psi/4 = \psi/4$ and $\theta = \psi/2$ as anticipated.

The Divergence Factor

There remains the consideration of the divergence factor. The argument in this case is essentially a geometrical one and all that really needs to be said is that in applying the above analysis the equivalent radius of the earth everywhere replaces the true value. The problem can thus be solved using straight ray paths as in I. However, it is instructive to use the above equations to obtain an alternative derivation of the divergence factor.

In Fig. 5, in addition to the indirect ray path TC and CR with the reflection point at C, there is shown a neighbouring ray that leaves the transmitter at an angle

τ below TC and strikes the earth at C′ at a distance ε ahead of C. The reflected ray then passes through R′ at a height δh_R above R. The quantities τ, ε and δh_R are limitingly small but have been greatly exaggerated in Fig. 5 for the sake of clearness.

In free space the corresponding width of the beam of angle τ at a distance d would be $d\tau$, and as there is no lateral deviation of the rays, the divergence factor D expressed in terms of relative amplitudes is

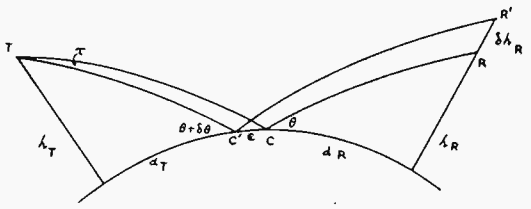

FIG. 5

$$D = \left[\frac{d\tau}{\delta h_R}\right]^{\frac{1}{2}} \tag{63}$$

restricting the argument to small values of the reflection angle θ.

Now for the ray TC, it has been seen that the elevation of the ray at T looking away from C is

$$\zeta = \theta + \frac{d_T}{r_e} \tag{64}$$

A neighbouring ray will be defined from equation (64) by

$$\delta\zeta = \delta\theta + \frac{\delta d_T}{r_e} \tag{65}$$

and for the particular ray TC′, $\delta\zeta = \tau$ and $\delta d_T = -\varepsilon$, so that from equation (65)

$$\tau = \delta\theta - \frac{\varepsilon}{r_e} \tag{66}$$

The appropriate value of $\delta\theta$ is decided by the fact that both rays pass through T, so that $\delta h_T = 0$, and from equation (49)

$$0 = d_T\,\delta\theta + \theta\delta d_T + \frac{d_T}{r_e}\,\delta d_T$$

Putting $\delta d_T = -\varepsilon$, this gives

$$\delta\theta = \left[\frac{\theta}{d_T} + \frac{1}{r_e}\right]\varepsilon \tag{67}$$

Thus from equations (66) and (67)

$$\tau = \frac{\theta\varepsilon}{d_T} \tag{68}$$

From equation (50) δh_R is given by

$$\delta h_R = d_R\,\delta\theta + \theta\delta d_R + \frac{d_R}{r_e}\,\delta d_R$$

For the ray C′R′, $\delta\theta$ is the same as in equation (67) and $\delta d_R = \varepsilon$, so that

$$\delta h_R = d_R\left[\frac{\theta}{d_T} + \frac{1}{r_e}\right]\varepsilon + \theta\varepsilon + \frac{d_R\,\varepsilon}{r_e}$$

which from equation (36) may be written

$$\delta h_R = \frac{d\,\theta\varepsilon}{d_T} + \frac{2d_R}{r_e}\varepsilon \tag{69}$$

Thus from equations (63), (68) and (69)

$$D = \left[1 + \frac{2\,d_T\,d_R}{r_e\,d\,\theta}\right]^{-\frac{1}{2}} \tag{70}$$

Equation (70) is equivalent to the value given in I with r_0 replaced by r_e and leads to the graphical method there derived for finding D.

If this proof is generalized to include all values of θ, great care has to be taken to include all terms of order $(d/r_e)\tan\theta$ relative to unity. In equation (63), d in the numerator must be replaced by a more accurate value of the length of the path TC + CR, and δh_R in the denominator must be multiplied by $\cos\zeta_R$, where ζ_R is the elevation of the ray CR at R, to take account of the fact that the normal to the ray makes an angle ζ_R with the vertical at R. Moreover, in differentiating the expressions for h_T and h_R to find $\delta\theta$ and δh_R in terms of ε, equations of the form in equation (35) must now be used. The final result is

$$D = \left[1 + \frac{2\,d_T\,d_R\sec^2\theta}{r_e\,d\tan\theta}\right]^{-\frac{1}{2}} \tag{71}$$

This result may be obtained by a simple generalization of the geometrical proof given in I.

When θ is small, equation (71) degenerates to equation (70), and when $\tan\theta$ is large it becomes

$$D = \left[1 + \frac{2\,d_T\,d_R\tan\theta}{r_e\,d}\right]^{-\frac{1}{2}} \tag{72}$$

Under the latter conditions $h_T \fallingdotseq d_T\tan\theta$ and $h_R \fallingdotseq d_R\tan\theta$, so that

$$D = \left[1 + \frac{2\,h_T\,h_R}{r_e\,(h_T + h_R)}\right]^{-\frac{1}{2}} \tag{73}$$

This result may be obtained by a simple geometrical proof for vertical incidence on a sphere of radius r_e.

The use of equation (35) instead of equation (29), which still contains r_0 explicitly, suggests that in equations (71) to (73) the use of r_e is not strictly correct. The point is, however, purely academic, since as θ is increased, D given by equation (70) becomes effectively unity while the approximation in equation (70) is still amply good. In fact, where expressions of the form in equations (71) and (72) have to be used in principle, D is always very close to unity. This is borne out by equation (73) where the difference of D from unity is clearly of the order of h/r_e, where h is the smaller of h_T and h_R, and is therefore negligible to the order of accuracy assumed throughout.

Conclusion

Although the results for small angles of elevation are well known, the presentation adopted has aimed at showing more clearly the nature of the approximations made in the analysis and the range of their validity. It will be noted that throughout the argument h_T and h_R are the actual heights above the true earth and not the equivalent

heights above the tangent plane at the reflection point. Similarly d_T and d_R are actual distances along the true earth.

In the transformed geometry, h_T and h_R are unaltered and become heights above the equivalent earth's surface drawn through the reflection point, which is positioned so that d_T and d_R remain unaltered although measured along the surface of the equivalent earth.

The angle of elevation at the reflection point derived from the transformed geometry is the true angle made by the curved ray paths with the actual earth's surface, which has to be used in finding the Fresnel reflection coefficient where it is significantly different from -1.

The only essential restriction imposed on the system is that the heights above earth are very small compared with the radius of the earth, a condition that is amply fulfilled for tropospheric propagation when a linear variation of refractive index with height can be assumed. The transformation is not formally confined to nearly horizontal rays, the true nature of it being to straighten the ray paths, whatever their direction relative to the horizontal, and hence whatever their curvature, may be. This generalization arises from the fact that in deriving equation (12) with the help of equations (7) and (8), the factor $\cos \zeta$ cancels out.

This investigation was prompted partly by the consideration of a transformation given in the Introduction to the new ground-wave propagation curves recently published by the C.C.I.R.[5] in which modified values of the dielectric constant and the conductivity of the earth are used in the geometric-optical formula within the horizon.

These values result from a transformation that uses the true radius of the earth and is expressed in terms of reduced heights and distances designed to connect with the reduced values used in the diffraction region. This use of such modified quantities, which are functions of the wave frequency, in the geometric-optical formula is presumably equivalent mathematically to the use of the equivalent earth radius concept, but it lacks its physical significance.

Such a transformation is probably more convenient when computing ground-wave curves very accurately near the horizon to join up with the curves obtained by taking a sufficiently large number of terms of the residue series used in the diffraction region. It is difficult, however, to see how such a transformation can be derived from a purely geometric-optical argument without recourse to a comparison with the form of the modification produced by the gradient of refractive index in the diffraction analysis.

The above treatment is a reassurance that in the geometric-optical region the usual method of transforming the geometry is essentially correct and general in its application, and is preferable for use where this region alone is under consideration.

References

[1] G. Millington. "Curved Earth Geometrical Optics." *Marconi Review* No. 80. 1946. Pp. 1-12.

[2] C. R. Burrows and S. S. Attwood. "Radio Wave Propagation." Academic Press Inc., Publishers. New York, N.Y. 1949.

[3] "Propagation of Short Radio Waves," edited by D. E. Kerr. Massachusetts Institute of Technology. McGraw-Hill Book Co. Inc.

[4] J. C. Schelleng, C. R. Burrows and E. B. Ferrell. "Ultra-short-wave Propagation." P.I.R.E. 21. 1933. Pp. 427-463.

[5] "Atlas of Ground-wave Propagation Curves for Frequencies between 30 Mc/s and 300 Mc/s." (C.C.I.R. Resolution No. 11), published by the International Telecommunications Union, Geneva, 1955.

A PRECISION ELECTRONIC SWITCH FOR FIXED COIL RADAR DISPLAYS

By A. P. Young and D. H. Chandler

Summary

The use of fixed coil deflection systems in radar displays allows operator controlled markers to be produced on the tube face. They are displayed between radar scans by switching between the time base and marker waveforms to produce a composite deflection waveform.

In order to maintain accurate correlation between the marker positions and the radar picture it was necessary to design an accurate and stable electronic switching unit.

During the design of this switching-circuit, difficulties were encountered due to the residual current in valves when in the cut-off state. The effect showed itself in two ways, first in producing imperfections in the switching action, and second in limiting the performance of a condenser store which was used to counteract D.C. drift in the switch. The solution of the first problem demanded the careful use of the properties of existing valves; that of the second involved the use of a non-linear silicon carbide resistor in an improved type of voltage store. The drift correction system is considered in detail, and the complete switch circuit is described.

1. Introduction

WHEN dealing with radar displays, a problem encountered is that of providing markers for the purpose of accurate measurement, or for application to remote indication and control. The fixed coil type of display is generally used because it permits the supply of all information to the tube face through a single deflection system, thus avoiding the uncertainties due to the superposition of two separate displays.

One method of displaying markers demands the production of two separate waveforms, one being the normal type of resolved radar timebase, and the other a complex waveform of D.C. levels switched sequentially by mechanical means. Each of these levels corresponds to the position of a marker, and each can be controlled by an operator. To each level is added a small waveform to give the marker a distinctive shape. It is then possible to combine these two waveforms electronically by a switching operation, such that the markers appear successively between timebase scans.

It is our purpose to describe the circuitry that has been developed to provide this switching action. It was designed for an accuracy approaching one part in ten thousand, involving a D.C. stability of about 5 millivolts.

2. The Basic Switching Element

The design was based on the simple switching element of Fig. 1. Here the switching waveform C is used to switch between the timebase A and the sequenced marker levels B to produce the output waveform D as shown in Fig. 2. Referring to Fig. 1, when the switching waveform C is at its lower level, the valve V5 is cut off, and the current in V6 is determined accurately by the value of R_k and by the potential

difference between the two negative H.T. lines. At the more positive level, V5 passes a known current and V6 is cut off. Thus, V5 acts as the " constant current " cathode load of the long-tailed pair V1 and V2 in one state, and V6 acts with V3 and V4 in the same way in the other state. Then the output waveform (Fig. 2D) consists of the resolved saw-tooth input, with marker voltages inserted during the rest periods.

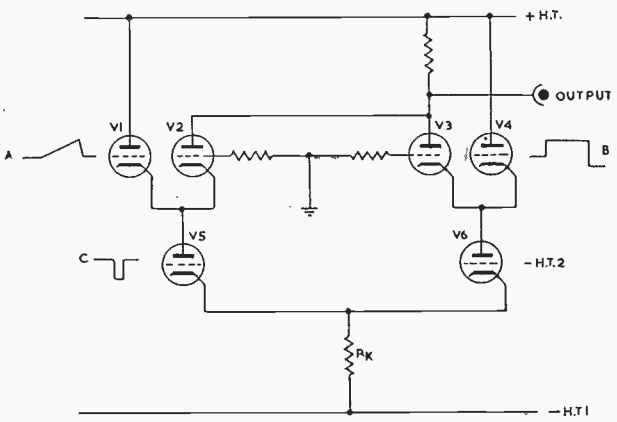

FIG. 1

The Basic Switching Element.

3. Interaction

In valves commonly supplied to industry, a residual current may be found, even when a large negative bias is applied to the grid. This is mainly because the cathode material is liable to extend beyond the region of effective grid control. This current is often appreciable compared with the normal working current of the valve. Taking for example three of the commonly used triodes, the figures are:—

	Typical working current	Specified maximum cut-off current
CV 4024	10 mA	10 μA
CV 4003	20 mA	20 μA
CV 4004	1 mA	35 μA

It is clear that the most favourable ratio that can be obtained is about 1000 : 1.

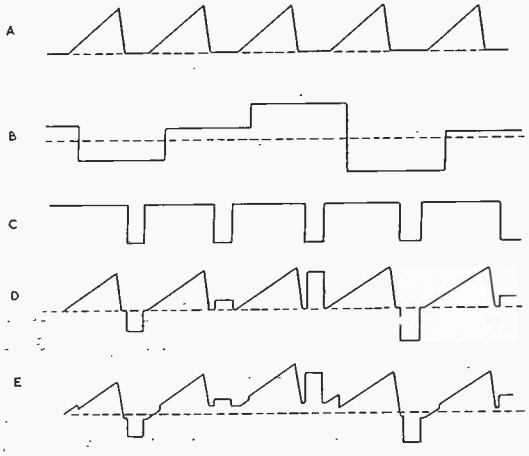

FIG. 2

Waveforms in the Switching Circuit.

A. Time base input.
B. Sequenced marker levels.
C. Switching pulse.
D. Desired output waveform from switch.
E. Output waveform from switch, showing imperfection due to residual currents.

This leakage current impairs the operation of the switch, as will be seen if we consider the effect of a residual current in V5 or V6 (Fig. 1). The output waveform is produced by the sum of the anode currents of V2 and V3, flowing in their common

anode load. The division of current between V1 and V2 is controlled by the grid of V1, and the grid of V4 has similar control over the current flowing in V3. Thus with V5 fully conducting, the current in the anode load is a proportion of the operating current of V5 plus a proportion of the residual current of V6. Then an attenuated version of the sequenced waveform will appear superimposed on the timebase waveform at the common anodes (Fig. 2E).

For example, if all valves were CV 4004, the cut-off current of V6 might be as high as 35 microamps, and this current might flow through either V3 or V4, depending on V4 grid potential. Now the transfer conductance from V1 grid to V2 anode is about 500 microamps per volt. Hence the signal at the anode is about the same as that which could be produced by 70 millivolts at V1 grid.

4. The Prevention of Interaction

Interaction can be overcome by connecting the two pairs of common cathodes through high resistances to a positive potential, as shown in Fig. 3. This ensures that the effect of leakage currents at the output is independent of the waveforms at V1 and V4 grids. An alternative source has now been provided which can supply the residual current for the switching valves. Referring to Fig. 3, with not more than 35 microamps flowing through V6, the potential of V6 anode cannot be more than 10 volts below the source voltage of 70 volts. The current variation in V4 cannot be greater than 35 microamps, and this change of current will not produce a change in the cathode voltage of V3 of more than 10 volts. But as this valve is cut off by at least 60 volts, its mutual conductance must be very small, and the interaction has become negligible.

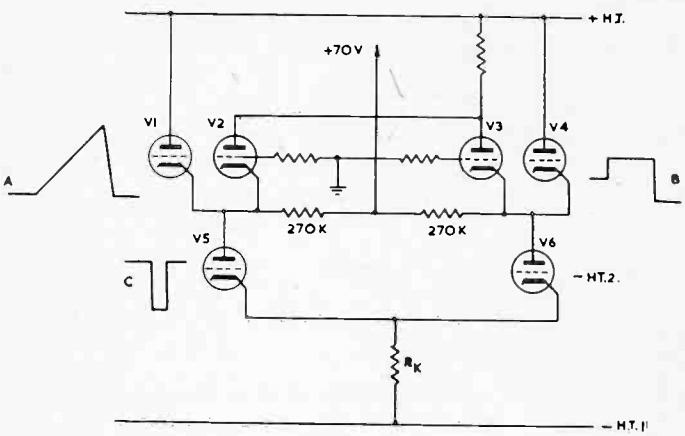

FIG. 3

The Basic Switching Element, modified to prevent interaction.

5. The Switch Incorporated in a Feedback Amplifier

To get the required linearity, it is necessary to apply negative feedback across the switch. We shall describe a circuit consisting of two D.C. coupled amplifiers of the see-saw type, where the addition takes place at the anode of the first stage, and the rest of the amplifier is common to both see-saws.

In this system the time-base waveform is applied at Y, and the sequenced waveform at X (Fig. 4). Due to the action of the switch, the output Z consists of the time-base waveform with samples of the sequenced waveform switched in between traces. The gain of each amplifier is unity, and there is the usual phase reversal between input and output. The waveforms have a range of +50 volts to −50 volts.

It was found that the use of a simple see-saw with capacitors connected directly across the see-saw arms introduced switching transients of long duration unless the resistive arms were inconveniently low. It was found preferable to include the cathode followers V7 and V8, which lowered the effective resistance of the see-saw arms and removed the need for trimming.

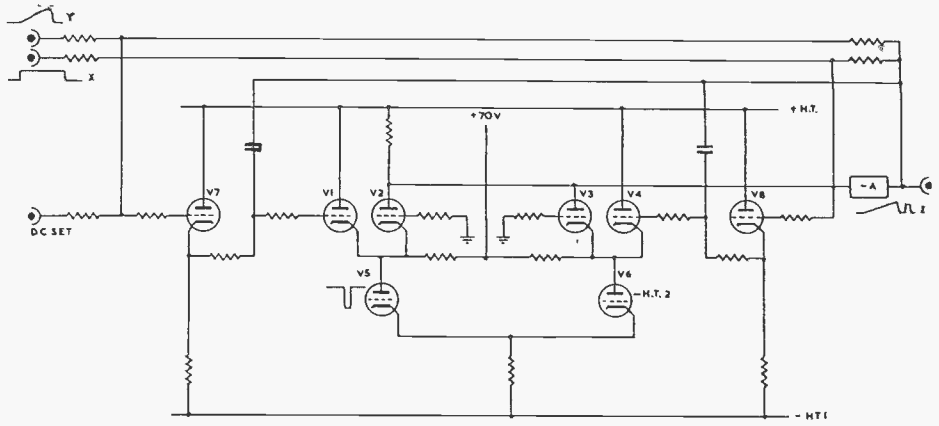

FIG. 4

The Switch, with overall feedback applied.

It should be noted that the type of feed-back capacitor used must be chosen carefully to avoid hysteresis effects. For example, plastic film capacitors are suitable.

6. D.C. Drift

A second failing of the simple switch is that of D.C. drift which changes the apparent D.C. levels of the waveforms A and B in Fig. 1. In our particular application, the only drift that is of importance is the difference between the drifts, for if the two levels drift in sympathy the accuracy of the marker system is unimpaired.

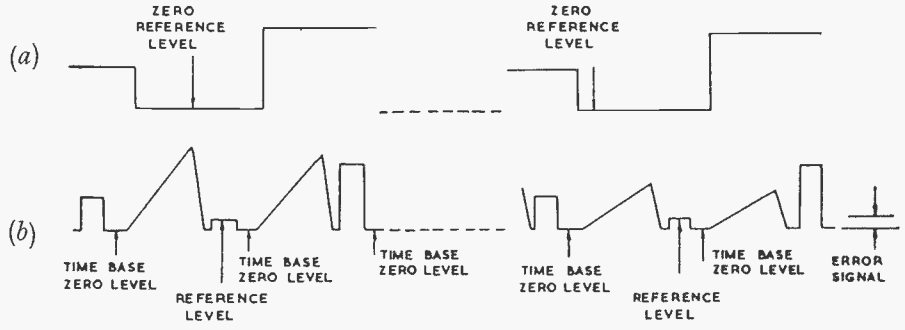

FIG. 5(A)

Sequenced marker levels with reference level inserted in one sequence.

FIG. 5(B)

Output waveform from switch showing time base with marker levels and reference level. The difference between the time base zero level and the reference level constitutes the error.

In our experience using stabilized heater and H.T. supplies, the day-to-day drift would be of the order of 30 millivolts, referred to grid level.

7. Automatic Zero Control

The object of the system of automatic zero control described here is to remove this relative drift. One of the marker sequences is used to inject into the amplifier a zero reference level to which the radar is set automatically (Fig. 5(a)). The " D.C. set " terminal of Fig. 4 is now connected to a store of the condenser type, whose input is controlled by an error signal obtained from the output waveform from the switch (Fig. 5(b)).

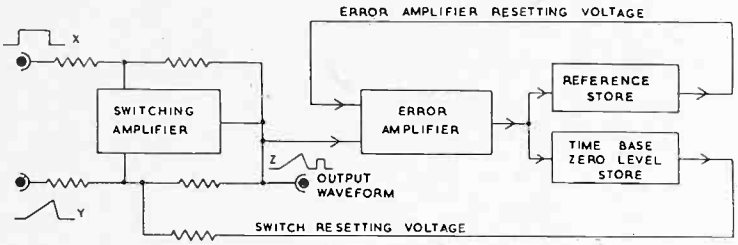

FIG. 6

System block diagram.

Since the two portions of the error information exist at different times, a continuous D.C. level must be produced to which both can be compared. This is the function of the reference store (Fig. 6). During the reference period, the reference store is corrected to the reference level; and during the time-base rest period, the time-base rest level is corrected to the reference store. By this means, the time-base rest level is corrected to the reference level.

Before describing the operation of the circuit more fully, we propose to explain why it was necessary to develop a special store for the automatic zero control system, and the mode of operation of the store.

8. Condenser Stores

The simplest type of condenser store is shown in Fig. 7. In order to store the peak level of the pulse shown applied at the input, the switch is closed during the period of the pulse, and during this time the condenser will take up the potential of the pulse top, provided the source potential is low enough. If the switch is opened before the end of the pulse, the condenser will remain at the same potential, which is that of the peak pulse voltage.

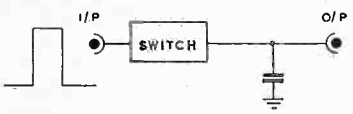

FIG. 7

Basic Condenser Store.

A simple development of this is shown in Fig. 8, where the store is included in a feedback circuit. When the switch is closed, the output takes up a level determined by the input, and maintains it after the switch is opened. In low speed applications, switching can be done mechanically, but in high speed applications the switching must be done electronically.

In electronic switches it is not possible to prevent leakage currents flowing into the condenser during the storage time. These currents cause the stored voltage to change, and reduce the accuracy of the device. In particular, it is clear that the

store will lose control if the charge that can be supplied to the condenser during the charging time is not greater than that which leaks away during the storage time, and in fact the quality of the store is largely determined by the ratio of storage current to leakage current. For a given accuracy the leakage current and storage time together determine the size of the condenser which must be used. The size of this condenser, together with the maximum available charging current, determine the speed of response. Hence for given storage and charging times, the product of speed and accuracy is directly proportional to the ratio of charging current to leakage current, and is independent of the condenser. This ratio can therefore be regarded as a figure of merit for such systems.

Where electronic valves are used in the switch, the best ratio that can be guaranteed is of the order of one thousand. Using diodes, it may be possible to do a little better, and typical figures are 30 milliamps to 15 microamps. In the case of electronic diodes, the leakage current is due chiefly to finite back resistance and to heater to cathode leakage.

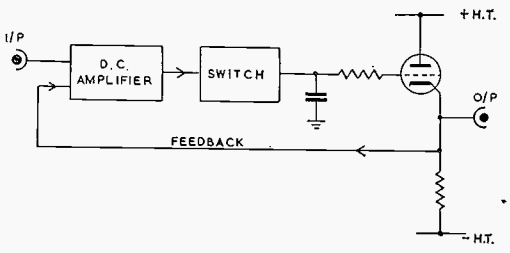

FIG. 8
Condenser Store with Feedback.

In our particular application, where the ratio of the storage time to the charging time was 400:1, and considerable accuracy and speed were required, ordinary electronic methods were not possible. It was therefore necessary to develop a store using a non-ohmic silicon carbide type of resistor. By this means we were able to guarantee a leakage current of less than 0·1 microamps, and charging currents of 50 milliamps or more would be permissible. The maximum charging current required in our application was about 5 milliamps, giving a figure of merit of about 5×10^4.

It will be seen that this figure is significantly better than can be produced by purely electronic means, and it can be rivalled only by the use of the recently developed type of crystal diodes.

9. Condenser Store Using Non-linear Resistor

In a condenser store, the quantities of importance are the impedance of the charging element and the voltage across it. In order to minimize the leakage current, it is desirable that during the storage time the impedance of the charging element should be as high as possible, and the voltage across it as small as possible. But during the charging time low impedance and high voltage are needed. In the case where a mechanical switch is used, the action results entirely from impedance changes. In the case where the condenser is charged through a linear resistance, the aim is to maintain zero voltage across the resistor during the storage time, and the action therefore depends entirely on voltage changes.

In the system which we are introducing here, advantage is taken of both of these factors, by using a charging element whose impedance varies with voltage.

The characteristic of the silicon carbide non-ohmic resistor used can be represented approximately by the relation

$$I \propto V^n$$

where I and V are the current and voltage respectively, and n is normally between 4 and 5 over a wide range of current densities. At low current densities the value

In our experience using stabilized heater and H.T. supplies, the day-to-day drift would be of the order of 30 millivolts, referred to grid level.

7. Automatic Zero Control

The object of the system of automatic zero control described here is to remove this relative drift. One of the marker sequences is used to inject into the amplifier a zero reference level to which the radar is set automatically (Fig. 5(a)). The " D.C. set " terminal of Fig. 4 is now connected to a store of the condenser type, whose input is controlled by an error signal obtained from the output waveform from the switch (Fig. 5(b)).

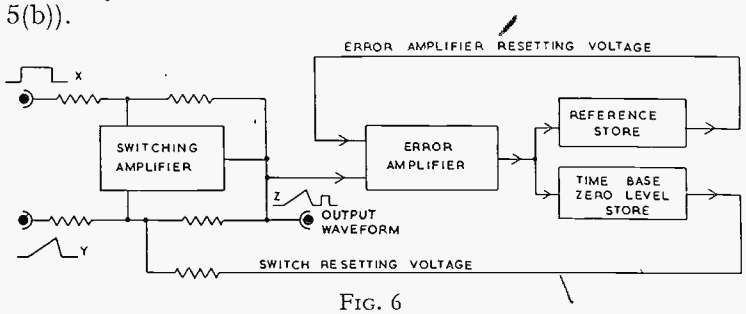

FIG. 6
System block diagram.

Since the two portions of the error information exist at different times, a continuous D.C. level must be produced to which both can be compared. This is the function of the reference store (Fig. 6). During the reference period, the reference store is corrected to the reference level; and during the time-base rest period, the time-base rest level is corrected to the reference store. By this means, the time-base rest level is corrected to the reference level.

Before describing the operation of the circuit more fully, we propose to explain why it was necessary to develop a special store for the automatic zero control system, and the mode of operation of the store.

8. Condenser Stores

The simplest type of condenser store is shown in Fig. 7. In order to store the peak level of the pulse shown applied at the input, the switch is closed during the period of the pulse, and during this time the condenser will take up the potential of the pulse top, provided the source potential is low enough. If the switch is opened before the end of the pulse, the condenser will remain at the same potential, which is that of the peak pulse voltage.

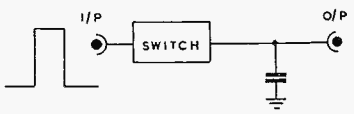

FIG. 7
Basic Condenser Store.

A simple development of this is shown in Fig. 8, where the store is included in a feedback circuit. When the switch is closed, the output takes up a level determined by the input, and maintains it after the switch is opened. In low speed applications, switching can be done mechanically, but in high speed applications the switching must be done electronically.

In electronic switches it is not possible to prevent leakage currents flowing into the condenser during the storage time. These currents cause the stored voltage to change, and reduce the accuracy of the device. In particular, it is clear that the

store will lose control if the charge that can be supplied to the condenser during the charging time is not greater than that which leaks away during the storage time, and in fact the quality of the store is largely determined by the ratio of storage current to leakage current. For a given accuracy the leakage current and storage time together determine the size of the condenser which must be used. The size of this condenser, together with the maximum available charging current, determine the speed of response. Hence for given storage and charging times, the product of speed and accuracy is directly proportional to the ratio of charging current to leakage current, and is independent of the condenser. This ratio can therefore be regarded as a figure of merit for such systems.

Where electronic valves are used in the switch, the best ratio that can be guaranteed is of the order of one thousand. Using diodes, it may be possible to do a little better, and typical figures are 30 milliamps to 15 microamps. In the case of electronic diodes, the leakage current is due chiefly to finite back resistance and to heater to cathode leakage.

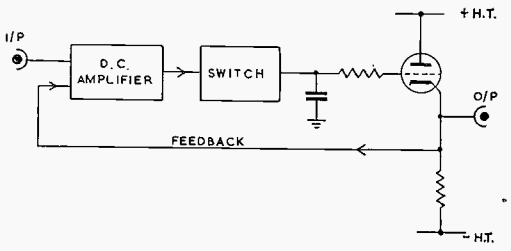

FIG. 8
Condenser Store with Feedback.

In our particular application, where the ratio of the storage time to the charging time was 400:1, and considerable accuracy and speed were required, ordinary electronic methods were not possible. It was therefore necessary to develop a store using a non-ohmic silicon carbide type of resistor. By this means we were able to guarantee a leakage current of less than 0·1 microamps, and charging currents of 50 milliamps or more would be permissible. The maximum charging current required in our application was about 5 milliamps, giving a figure of merit of about 5×10^4.

It will be seen that this figure is significantly better than can be produced by purely electronic means, and it can be rivalled only by the use of the recently developed type of crystal diodes.

9. Condenser Store Using Non-linear Resistor

In a condenser store, the quantities of importance are the impedance of the charging element and the voltage across it. In order to minimize the leakage current, it is desirable that during the storage time the impedance of the charging element should be as high as possible, and the voltage across it as small as possible. But during the charging time low impedance and high voltage are needed. In the case where a mechanical switch is used, the action results entirely from impedance changes. In the case where the condenser is charged through a linear resistance, the aim is to maintain zero voltage across the resistor during the storage time, and the action therefore depends entirely on voltage changes.

In the system which we are introducing here, advantage is taken of both of these factors, by using a charging element whose impedance varies with voltage.

The characteristic of the silicon carbide non-ohmic resistor used can be represented approximately by the relation

$$I \propto V^n$$

where I and V are the current and voltage respectively, and n is normally between 4 and 5 over a wide range of current densities. At low current densities the value

of n decreases, and over our working range of current (between 0·1 microamp and 5 milliamps) the effective value of n is about 3. The characteristic is roughly symmetrical, and the current reverses when the applied voltage is reversed. A typical characteristic is shown in Fig. 9.

In the storage condition the voltage across the resistor is less than 1 volt, ensuring a leakage current of less than 0·1 microamp. During the charging time, 60 volts across the resistor ensures a charging current of at least 5 milliamps. These figures allow a reasonable safety margin.

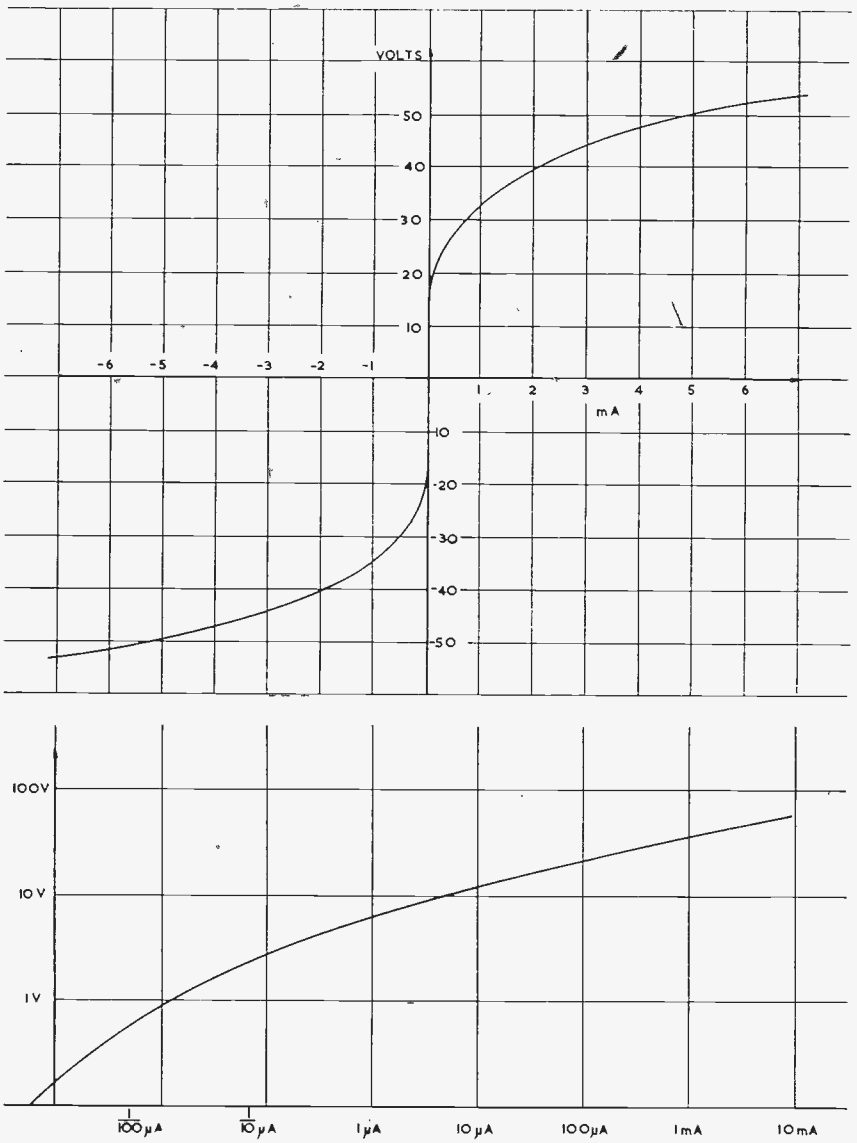

FIG. 9
Characteristic of typical non-linear Resistor.

10. The Complete Storage Circuit

The difference between the potential of the storage condenser and the potential required there can be used to provide an error signal. To reduce the error to a satisfactory value, it is necessary to provide a large charging voltage until the error approaches this value. This also results in the maximum possible rate of charge. The type of charging action described is obtained by including the store in a feedback amplifier having a suitably high loop gain. The system is shown in Fig. 10.

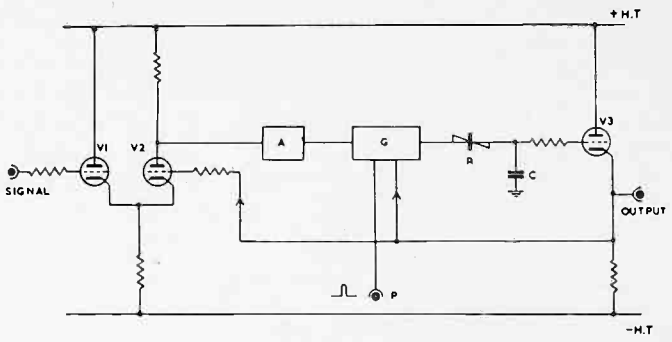

FIG. 10
Store using non-linear Resistor.

In this circuit, the stored output appears at V3 cathode, and is fed back to V2 grid. Then the signal at V2 anode is an amplified version of the difference between the input signal and the stored output level. This signal is further amplified in the D.C. amplifier A and is applied to the gate G. During the storage time, the output voltage from the gate is substantially equal to that at V3 grid. During the charging time, a pulse is applied to the terminal P of the gate G, which now connects the output of the amplifier A to the store. Thus during the charging time, the potential of V3 cathode moves steadily until there is little voltage across the charging element R. At this stage the output potential has reached the desired value.

The storage circuit is shown in detail in Fig. 11. In this figure valves 1 to 4 constitute a high gain D.C. amplifier; and it will be observed that these stages are of the "non-blocking" type, in the sense that none of these valves is driven into grid current by signals of normal amplitude. V5 and V6 together constitute a similar stage which operates only when V7 is conducting. During the storage time, V8 is conducting and V7 is cut off. The switching action is controlled by a small negative pulse applied to V8 grid during the charging time, and the action of the switch will be recognised as a simple variant on that described in paragraph 4 above. On switching, a pulse appears at V6 anode whose amplitude and sign depend on the potential at V5 grid. The values of the three resistors in V8 anode circuit are arranged such that the potential at V6 anode during the storage time is the mean of the extreme values it can take during the

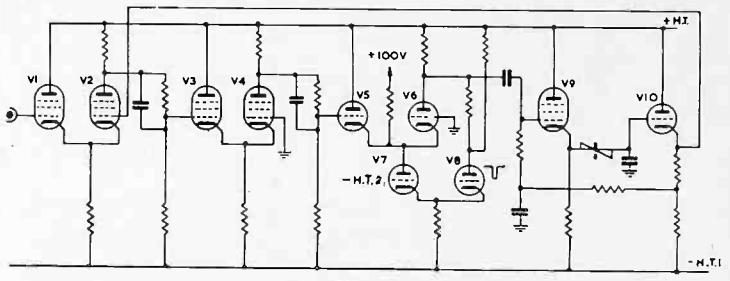

FIG. 11
Complete Storage Circuit.

charging time. The pulse is applied through an A.C. coupling and a cathode follower to the charging element, and current is thus supplied to the condenser in such a sense as to cause the pulse amplitude to be reduced by the feedback to V2 grid. The D.C. conditions of valves V9 and V10 are so arranged that in the time between pulses a very small potential appears across the non-ohmic resistor. The design centre

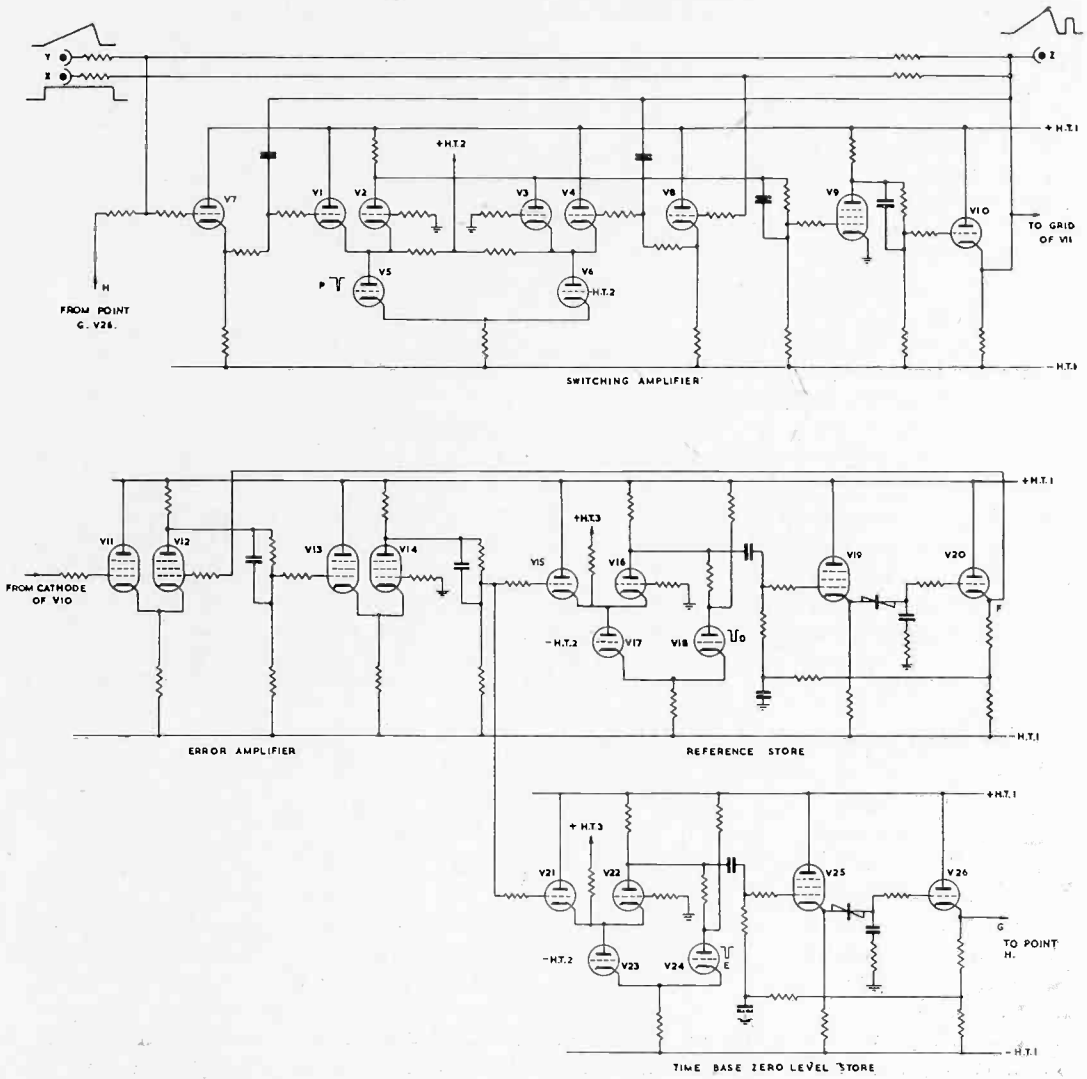

FIG. 12

Circuit diagram of complete system.

for this potential difference is zero, and it cannot exceed about one volt even with adverse component tolerance. The corresponding leakage current through the non-ohmic resistor determines the limit to the performance of the store in this respect.

It will be seen that a small pulse must be applied to the charging element at each charging time to supply the charge that leaks away during the storage time. The gain of the preceding amplifier is determined by the size of this pulse and the accuracy required.

In order to ensure correct working of the amplifier, the values of the compensating capacities used in the D.C. couplings must be carefully chosen, or the resistor values must be kept small. This ensures that any transients in the amplifier are small and short-lived—an essential feature, since the amplifier frequently runs into limit during the storage time.

The stability of a circuit of this form can be analysed by the use of the "describing function" technique. This consists in analysing the circuit performance for sine-waves of various amplitudes, ignoring the effects of harmonics produced by the non-linear element, as these are normally unimportant. In our case, only the largest signal amplitude need be considered. When the circuit is found to be unstable, this can usually be remedied by providing some phase advance in the storage circuit or later. A small resistance placed in series with the storage condenser has been found effective.

11. The Complete Circuit

Fig. 12 shows a complete circuit diagram of the system. The time-base waveform is injected at Y, the sequenced marker levels at X, and the switching waveform at P. Valves V1 to V10 constitute the main switching circuit, which was described earlier. The error amplifier for the automatic zero control storage systems consists of valves V11 to V14, and feeds the two gating stages which control the stores. The gating stage of the reference loop is operated during the time of the reference marker by the pulse applied at D. The gate of the correction loop is operated by the pulse at E during each rest period of the time-base. The two stored voltages appear at F and G.

It will be seen that when these voltages have reached steady values, the pulses applied to the non-linear resistances must both be small. This implies that the grids of valves V15 and V21 are close to earth during their respective gating periods. Hence the reference level and the rest level in the waveform applied to the error amplifier can differ only by a very small amount and correction has been achieved.

Acknowledgments

The authors wish to stress that many features of the design arose out of discussions with other members of the Radar Research Group.

We wish particularly to acknowledge the many helpful suggestions made by Mr. R. B. Donaldson, and by Messrs. R. P. Shipway & A. B. Starks-Field who directed the work.

Our thanks are also due to the Ministry of Supply for permission to publish this paper.

AN EXPERIMENTAL AIRBORNE TELEPRINTER SERVICE FOR NORTH ATLANTIC AIRLINES

By A. Bickers, B.Sc.(Eng.)

This article discusses the desirability of a ground to air teleprinter service for aircraft flying on the North Atlantic route. A description of an experimental receiving installation designed by the Marconi Company is given together with some details of the receiving equipment. System parameters are considered with particular reference to the carrier frequencies involved and a typical example is given to show the order of frequency shift which is needed on a system of this kind. A brief summary is included of the results so far obtained; results which in themselves are sufficient to show that an airborne teleprinter service for the North Atlantic is a very realistic proposition.

Introduction

RADIO communication between two aircraft, and between aircraft in flight and the ground, is carried out where possible in the band of 100-150 Mc/s. Unfortunately, range is limited to line-of-sight or just beyond, and will depend largely upon the height of the aircraft concerned. Beyond the range of V.H.F. communications it is necessary to resort to the medium and high frequency bands between 300 kc/s and 30 Mc/s, where ranges up to 2,000 miles either on R.T. or C.W. are made possible by sky wave propagation. Aircraft flying on the North Atlantic route are out of range of land on V.H.F. for most of the flight and except for landing information, all traffic is at present handled by the M.F. and H.F. bands, resulting in a great deal of radio congestion.

A recent survey made by a group of North Atlantic Air Line operators showed that a very large proportion of the time available on the overcrowded M.F. and H.F. radio bands was taken up by the transmission of weather information. This has meant that other signals are frequently delayed. Moreover, bad transmissions due to unfavourable sky wave conditions on these bands have resulted in the loss of much-needed weather information by aircrew flying over mid-Atlantic. The solution appeared to lie in the provision of a ground-to-air meteorological service which could supply all the necessary weather information and which would operate reliably even when conditions cause transmission failures on high frequencies.

Consideration of available bandwidths, sending speeds, crew operating requirements, etc., all suggested an automatic ground-to-air telepriner service transmitted on the long-wave band. Such a service would also afford a welcome alleviation for normal traffic on the H.F. band.

A number of companies interested in the production of airborne communications equipment including the Marconi Company, have been invited by the NARTEL organization to produce experimental receivers for installation in aircraft which are already in service on the North Atlantic route in order to prove the effectiveness of the system and the various performance estimates which have been made.

General description of the Airborne Receiving Equipment

The Marconi airborne teleprinter receiver X2779 has been produced in accordance with these requirements. It supplies line current to a Creed Model 75 teleprinter (Fig. 1) weighing approximately 35 lbs. which has been specially adapted for airborne purposes.

The wireless equipment comprises a receiver of dimensions 6 inches by 8 inches by 15½ inches weighing 19 lbs., a control unit 2 inches by 2 inches by 3½ inches for remote switching and channel selection, a small open wire aerial 4½ feet long spaced approximately 17 cm from the underside of the aircraft and an aperiodic amplifier 3 inches by 3 inches by 4½ inches located inside the aircraft skin as near as possible to the aerial lead-through. Later on an anti-static omnidirectional loop aerial may be available, so that the equipment will become less susceptible to nearby electrical disturbances. The various units are interconnected through the back plate junction box X2384.

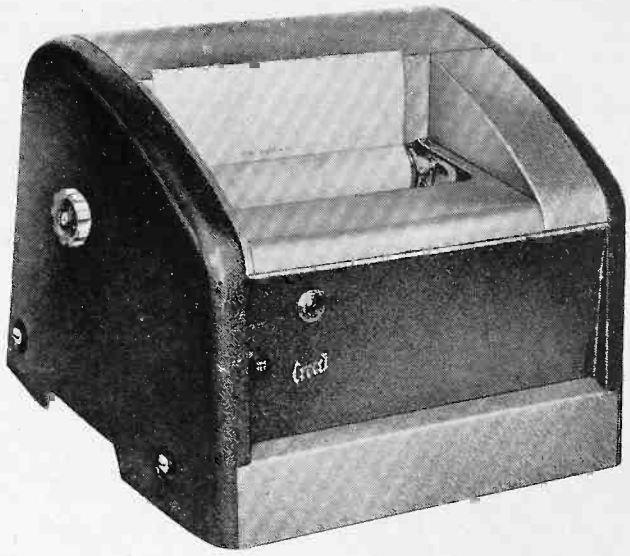

FIG. 1

The Creed Model 75 Teleprinter.

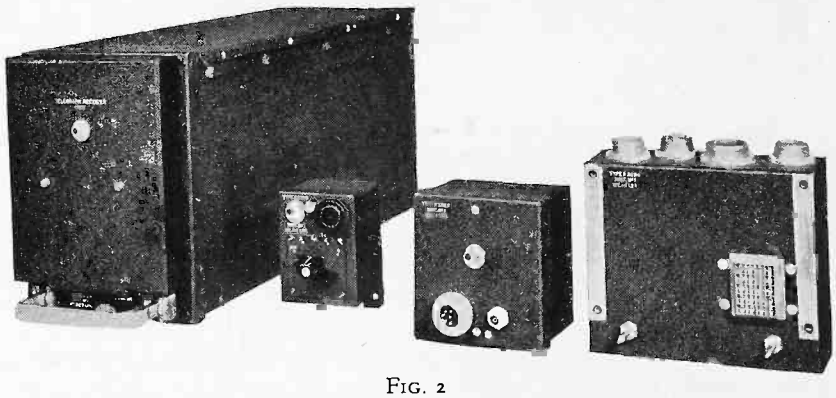

FIG. 2

The units of the airborne receiving installation showing left to right the receiving unit, control unit, aperiodic aerial amplifier and the back plate junction box.

In order to facilitate the type of investigation and modification work which is inevitable on experimental equipment the present model has been designed so that the complete receiving chassis and the power supply unit may be easily removed

from the main housing. Plug-in connections are used throughout. The receiving chassis is also arranged so that all trimming operations including channel tuning and crystal setting may be carried out from the front of the set. These arrangements are illustrated in Figs. 2, 3, 4 and 5.

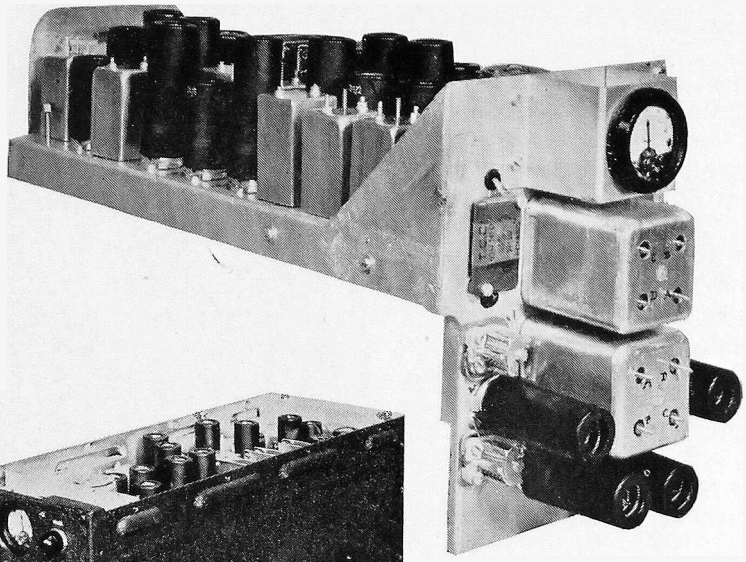

FIG. 3

The complete receiver chassis removed from the housing.

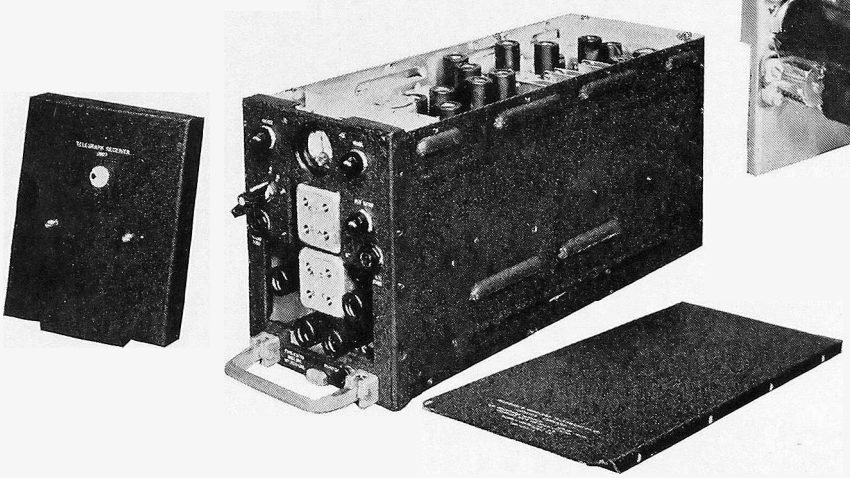

FIG. 4

The complete receiving unit with the receiving chassis in position. The power unit is situated in the lower portion of the main housing.

The receiver is crystal controlled and is designed for frequency shift keying on any one of four channels in the range 90-130 kc/s. It is remotely controlled from any suitable position in the aircraft and will function on narrow shift keying with any value of shift between 40 c/s and 80 c/s at speeds up to 75 bauds (approx. 100 W.P.M.). A double current output for the teleprinter is available up to ± 25 mA.

The small signals picked up by the open wire aerial may be considered as being derived from a high capacitive-reactance source. In order to bring these signals from the aerial to the input of the receiver, it is necessary to lower the impedance to that of a suitable co-axial line, and for this purpose the aperiodic aerial amplifier is employed. It is essentially an impedance transforming device with added gain in order to reduce effective receiver noise.

Permeability tuning is employed to tune the signal frequency stages of the receiver. The coils are mounted in two groups of four inside aluminium screening

cans (Fig. 3). Automatic and remote selection is achieved by the employment of the Ledex type motor operating a bank of switch wafers which select the appropriate coil and crystal. Each coil is tunable over the whole frequency range so that any combination of four channels may be selected.

The mixer, with its stable crystal controlled oscillator, is followed by an intermediate frequency amplifier working at 85 kc/s. It consists of two parts, the first of

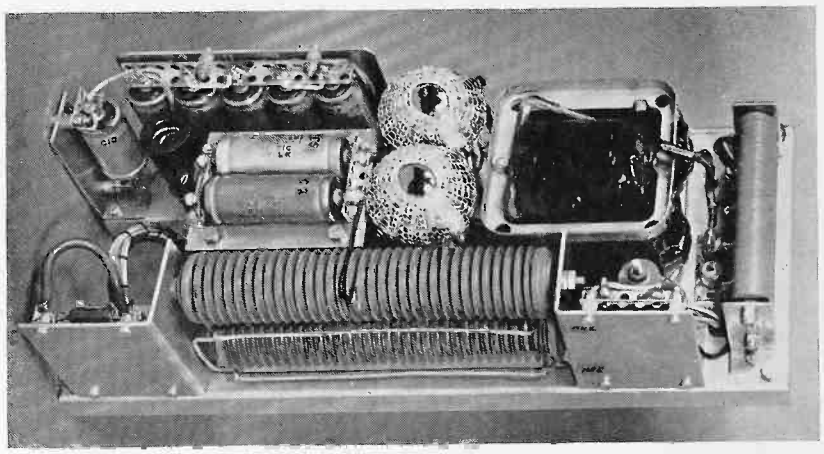

FIG. 5

The power unit removed from the main housing.

which is comparatively broad-band and operates a short time-constant amplified A.G.C. which can effectively limit the amplitude of short duration interference pulses at the input to the second part of the amplifier which is highly selective. This selectivity is at present provided by a two-stage crystal lattice filter which if excited by interference pulses would ring and disable the receiver long after the originating pulse has disappeared. Additional gain with A.G.C. is available in the second part of the I.F. amplifier so that should a strong adjacent channel operate the A.G.C. in the early stages, the resultant loss of gain can be compensated.

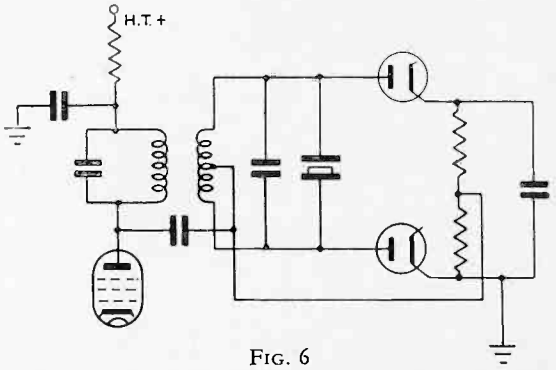

FIG. 6

Circuit diagram of the "crystal controlled" Foster Seeley discriminator.

It is to be expected that any benefits which may be derived from this arrangement would occur under marginal conditions of pulse interference. In order to obtain marked improvements from a system of this kind, a delay line would have to be inserted between the crystal filter and the output of the first I.F. amplifier. Unfortunately the added bulk of a delay line would at the present time be uneconomical for airborne purposes. The need for a signal strength indicator with linear indication

of signal strength from the narrow band filter has further compromised this part of the system which would ideally give a constant output irrespective of input above a predetermined level.

Demodulation, after a single stage amplitude limiter, is achieved with a Foster Seeley discriminator circuit, modified to include a crystal resonator to give a steep

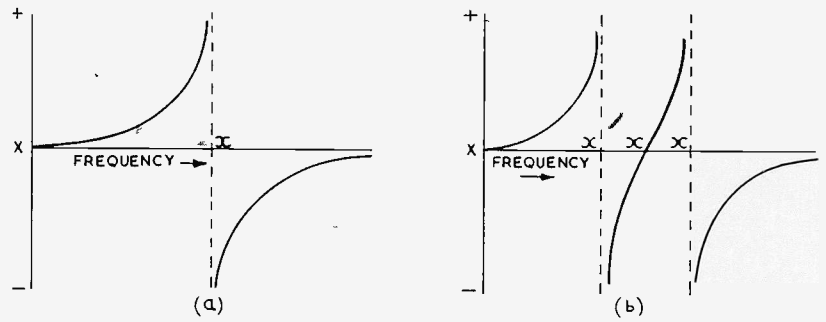

FIG. 7

Reactance charts for (a) the Foster Seeley discriminator, compared with (b) the "crystal controlled" version.

amplitude-frequency characteristic. The arrangement is shown in Fig. 6. It will be seen that a quartz resonator, cut so that its series resonant frequency is at the centre frequency of the discriminator, has been connected in parallel with the secondary tuned circuit. The reactance chart of the secondary circuit is now of the form shown in Fig. 7b instead of the one which applies to the usual Foster Seeley arrangement illustrated in Fig. 7a. So long as the phase of the secondary emf relative to the primary is 90°, or the amplitude is zero, the diodes will rectify emf's of equal or zero

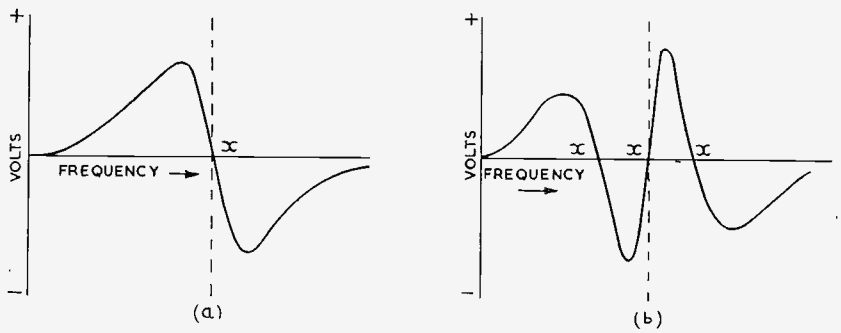

FIG. 8

Output characteristics for (a) the Foster Seeley discriminator compared with (b) the "crystal controlled" version.

amplitude, the resultant output being zero. Referring to Figs. 7a and 7b such points are marked at X. The resulting discriminator characteristics are shown in Figs. 8a and 8b.

The advantages of this modified version of discriminator lie in the sensitivity, which may be as high as two volts/cycle/second at 85 kc/s, and also in the fact that the centre of the discriminator is set exactly by the series resonant frequency of the crystal. Any misadjustment of the primary circuit will lower the amplitude, while misadjustment of the secondary produces asymmetrical sensitivity.

The telegraph bridge is included on the receiver chassis. Essentially the bridge is a direct coupled limiter/amplifier, which incorporates a low pass filter so that only the fundamental of the keying frequency is accepted. Thus an amplified strip is cut from the very centre of the detected signal to actuate a trigger circuit and feed steep fronted pulses of current to the electro-magnet of the teleprinter (Fig. 9). The steepness of the leading edge and the peak value are determined by the constants of the source and teleprinter coil circuit. Noise interference alters the mark-space ratio and will ultimately cause the teleprinter to misprint.

Power supplies come from the plug-in power unit contained in the lower portion of the main receiver housing, Fig. 5. The switch motor operates from the aircraft 28V supplies, from which current is required during channel selection only. All the normal supplies come from the power pack which operates from the aircraft 400 c/s 115 volt inverters. The power pack provides normal filament power and in addition a positive unstabilized 160 volt line, a positive stabilized 150 volt line and negative stabilized 150 volt and 230 volt lines.

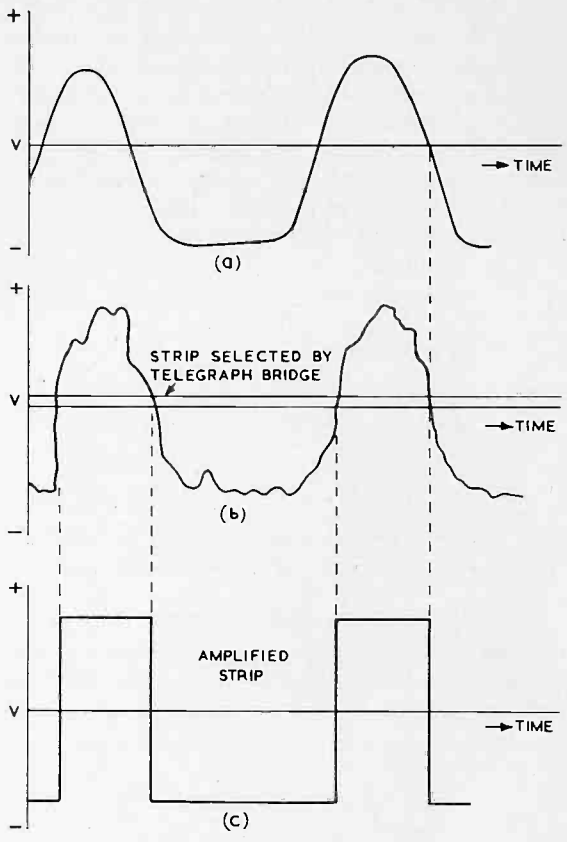

FIG. 9

(*a*) *Fundamental FSK signal without noise.*
(*b*) *Discriminator output with noise.*
(*c*) *Teleprinter current.*

Choice of Parameters for the Keying System

One of the problems set by the inauguration of a service of this nature lies in the choice of a suitable value for the frequency shift.

A wrong decision here can easily affect the range of service to the extent of many minutes of flying time, or alternatively increase the necessary transmitter power by several hundred watts.

In general, the emf picked up by the aerial contains the wanted signal, many unwanted signals and noise. To these are added receiver noise. The unwanted signals are filtered out by means of the selective circuits of the receiver leaving amplified signal plus noise, at the input terminals of the limiter. The amplitude of the noise is dependent upon the bandwidth of the selective circuits and this in turn depends upon the value of frequency shift adopted by the system and the extent to which harmonics of the keying frequency are retained. In general the bandwidth

required for the I.F. amplifier B_{IF} will be equal to the total frequency shift plus twice the fundamental of the keying frequency, or

$$B_{IF} = 2(\triangle f + f_k) \tag{1}$$

$\triangle f$ is the frequency deviation and is half the total shift. f_k is the fundamental of the keying frequency. Only the fundamental of the keying frequency is retained as any advantage in working with a rectangular wave is lost by the increase in bandwidth needed where noise is the limiting factor. Amplitude variations due to noise are now removed by the limiter. Frequency modulated noise will appear with the detected signal but A.M. noise will have been removed. Thus an improvement in signal to noise ratio will have been effected as a result of passing the signal through the limiter circuit. This improvement P in signal to noise ratio is given by

$$P = \frac{3\triangle f^2 B_{IF}}{2B_{LF}{}^3} \tag{2}$$

If
$$B_{LF} = f_k \tag{3}$$

from (1), (2), (3)

$$P = 3m^2 (1 + m) \tag{4}$$

B_{LF} = Low Frequency pass band.
B_{IF} = I.F. pass band.
m = Modulation Index = $\triangle f / f_k$
P is expressed as a power ratio.

The peak to r.m.s. ratio of white noise is generally accepted as being about 4 : 1 and the peak to r.m.s. ratio of the carrier is $\sqrt{2} : 1$. In order to prevent any amplitude variations from "breaking through" the limiters it is necessary for the value of peak carrier to be greater than peak noise. This means that the minimum signal

FIG. 10

a. Original limit of permissible noise fluctuation on signal.

b. Limit of permissible noise fluctuation after drift.

d. Total frequency drift.

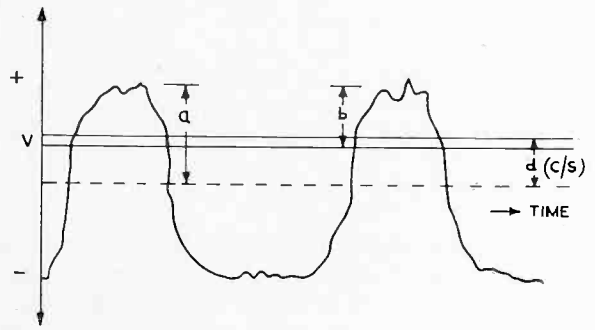

to noise ratio before the limiter must be greater than $\left(\frac{4}{\sqrt{2}}\right)^2$ i.e. 9 dB. In practice this threshold value will be nearer to 12 dB, depending on the efficiency of the limiters.

The system parameters will now be determined by the minimum improvement in signal to noise ratio p above the threshold value which is necessary for the telegraph bridge to operate the teleprinter correctly. The signal to noise ratio required at the input of a regenerative type of telegraph bridge will be the same as that needed to operate the pre-detector limiter, i.e. $P = 1$. This assumes an ideal bridge and

absolute frequency stability which cannot be achieved in practice. If we refer to Fig. 10 it can be seen that a drift of d c/s in the total system between transmitter and discriminator will result in the need for a value of P which is greater than unity.

Furthermore, a direct printing bridge will need at least 33% of the signalling element near the centre to be free of noise.

Assuming that only the fundamental of the keying frequency is accepted it may be shown that

$$P = \frac{\Delta f^2}{\left|\frac{\nu 3}{2}\Delta f - d\right|^2} \tag{5}$$

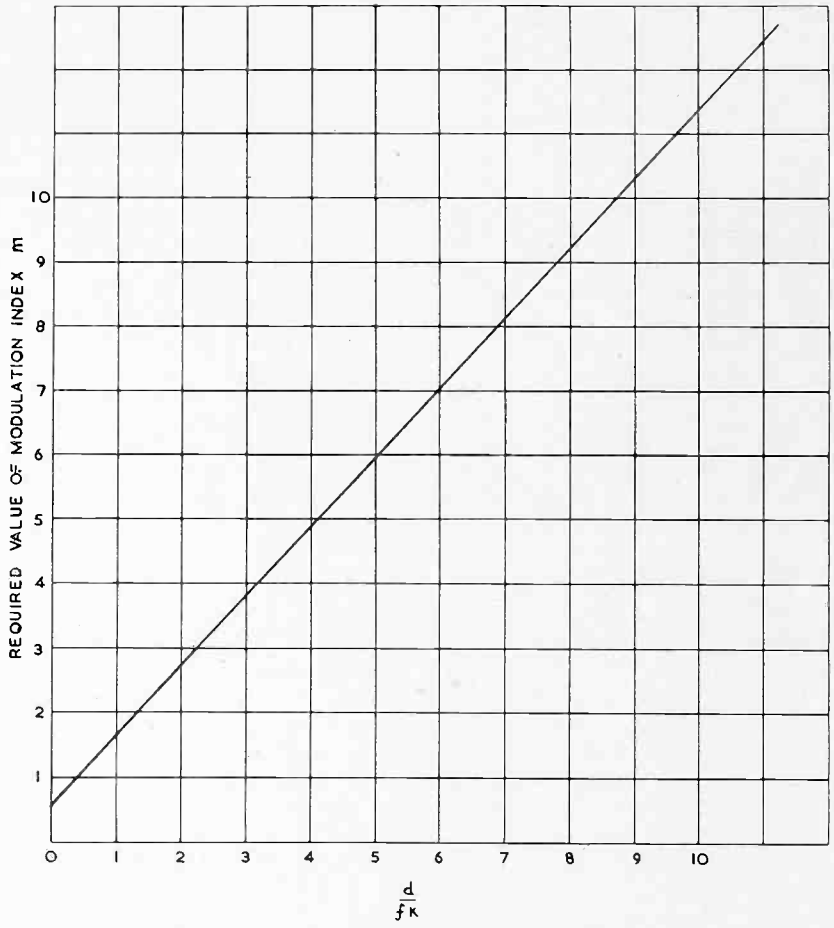

FIG. 11

The graphical solution of equation 6.

Combining equations (4) and (5) gives

$$\frac{9}{4}m^3 + m^2\left(\frac{9}{4} - 3\sqrt{3}\frac{d}{f_k}\right) + m\left(3\frac{d^2}{f_k{}^2} - 3\sqrt{3}\frac{d}{f_k}\right) + \left(3\frac{d^2}{f_k{}^2} - 1\right) = 0 \tag{6}$$

required for the I.F. amplifier B_{IF} will be equal to the total frequency shift plus twice the fundamental of the keying frequency, or

$$B_{IF} = 2(\triangle f + f_k) \tag{1}$$

$\triangle f$ is the frequency deviation and is half the total shift. f_k is the fundamental of the keying frequency. Only the fundamental of the keying frequency is retained as any advantage in working with a rectangular wave is lost by the increase in bandwidth needed where noise is the limiting factor. Amplitude variations due to noise are now removed by the limiter. Frequency modulated noise will appear with the detected signal but A.M. noise will have been removed. Thus an improvement in signal to noise ratio will have been effected as a result of passing the signal through the limiter circuit. This improvement P in signal to noise ratio is given by

$$P = \frac{3\triangle f^2 B_{IF}}{2B_{LF}^3} \tag{2}$$

If
$$B_{LF} = f_k \tag{3}$$

from (1), (2), (3)

$$P = 3m^2 (1 + m) \tag{4}$$

B_{LF} = Low Frequency pass band.
B_{IF} = I.F. pass band.
m = Modulation Index = $\triangle f / f_k$
P is expressed as a power ratio.

The peak to r.m.s. ratio of white noise is generally accepted as being about 4 : 1 and the peak to r.m.s. ratio of the carrier is $\sqrt{2} : 1$. In order to prevent any amplitude variations from "breaking through" the limiters it is necessary for the value of peak carrier to be greater than peak noise. This means that the minimum signal

FIG. 10

a. Original limit of permissible noise fluctuation on signal.

b. Limit of permissible noise fluctuation after drift.

d. Total frequency drift.

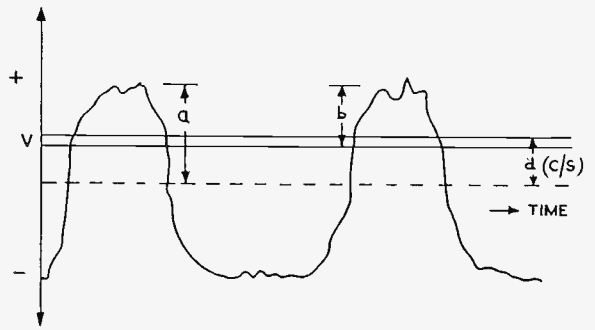

to noise ratio before the limiter must be greater than $\left(\frac{4}{\sqrt{2}}\right)^2$ i.e. 9 dB. In practice this threshold value will be nearer to 12 dB, depending on the efficiency of the limiters.

The system parameters will now be determined by the minimum improvement in signal to noise ratio p above the threshold value which is necessary for the telegraph bridge to operate the teleprinter correctly. The signal to noise ratio required at the input of a regenerative type of telegraph bridge will be the same as that needed to operate the pre-detector limiter, i.e. $P = 1$. This assumes an ideal bridge and

absolute frequency stability which cannot be achieved in practice. If we refer to Fig. 10 it can be seen that a drift of d c/s in the total system between transmitter and discriminator will result in the need for a value of P which is greater than unity.

Furthermore, a direct printing bridge will need at least 33% of the signalling element near the centre to be free of noise.

Assuming that only the fundamental of the keying frequency is accepted it may be shown that

$$P = \frac{\Delta f^2}{\left[\frac{\nu 3}{2}\Delta f - d\right]^2} \tag{5}$$

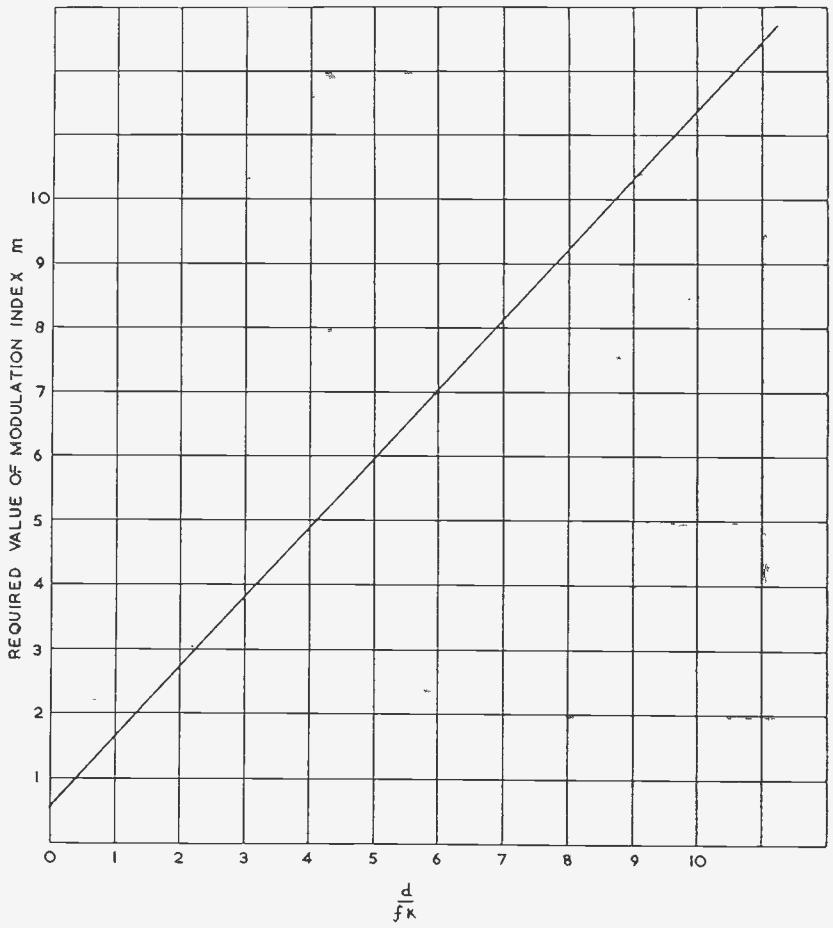

FIG. 11

The graphical solution of equation 6.

Combining equations (4) and (5) gives

$$\frac{9}{4}m^3 + m^2\left(\frac{9}{4} - 3\sqrt{3}\frac{d}{f_k}\right) + m\left(3\frac{d^2}{f_k{}^2} - 3\sqrt{3}\frac{d}{f_k}\right) + \left(3\frac{d^2}{f_k{}^2} - 1\right) = 0 \tag{6}$$

Equation (6) has been solved graphically and values of m plotted in terms of d/f_k are given in Fig. 11.

In the case of the experimental North Atlantic Teleprinter service, the transmitter stability is $\pm$ 1 c/s, the receiver oscillator stability $\pm$ 8 c/s, the discriminator stability $\pm$ 3 c/s and the equivalent drift of the telegraph bridge $\pm$ 2 c/s, giving a total effective drift of $\pm$ 14 c/s. The keying speed has been arbitrarily taken as 45·5 bauds, i.e. f_k=22·75 c/s. Thus $d/f_k = 0{\cdot}615$ showing, from Fig. 10 a required value of modulation index of 1·22 and a shift of 55·5 c/s. It is considered however that the drift figures stated are not large enough to account for all contingencies likely to be met in practice and it is probable that a larger value of shift will eventually be chosen.

The Transmitters

It is intended to install two permanent transmitters, near the coast on each side of the Atlantic. The estimated power requirements are something in excess of 2 kW radiated. At present the station on the Europeon side is an M.T.C.A. Station MYB on 121·6 kc/s at Galdenoch near Stranraer, Scotland, but it is only radiating 1 kW for the experimental period. On the Western side of the Atlantic another temporary station has been set up by T.C.A. at Chatham in Canada. It is transmitting 2 kW on 118·8 kc/s, but is sited some 500 miles inland. A variety of practical considerations have temporarily dictated a shift as low as 40 c/s. Thus the experimental transmitting system falls far short of what is believed to be the minimum for a satisfactory service.

Conclusions

The service has been in experimental operation since the beginning of March 1956. To date, approximately 50 crossings have been made with the receiving installations of three different communications companies. Correct printing has been possible at ranges exceeding 700 nautical miles from Galdenoch by day over a sea path where the field strength falls to a few microvolts per meter. By night, quite a lot of sky wave interference has been observed, resulting in fairly sharp minima for short periods when the ground and sky waves are comparable and in anti-phase. During these periods outages occur if the general level of field strength is low, as at about 30°W.

Complete outages are occurring when the aircraft flies through zones of static electrical interference, but it is hoped and expected that the use of an anti-static balanced loop aerial will reduce outages due to this effect. One of the installations is already fitted with an anti-static loop, but it is too early to make any assessment of the relative virtues of the two types of aerial, as it is not possible to have the two installations flying in the same area at the same time. A statistical assessment will be made on completion of the present series of tests.

In general, the results agree very well with the earlier predictions and have been most encouraging. There seems little doubt that the long-wave teleprinter service will, in spite of the added weight involved, become a permanent feature of North Atlantic Airline Communications.

Acknowledgments

The author wishes to express his thanks to Dr. G. L. Grisdale for his help and advice in the preparation of this article and to those members of the Communications Research Group of Marconi's Wireless Telegraph Co. Ltd. who helped in the design and construction of the equipment. Thanks are also due to Creed & Co., Ltd., for permission to illustrate their model 75 Teleprinter.

MARCONI'S WIRELESS TELEGRAPH COMPANY, LIMITED

ASSOCIATED COMPANIES, REGIONAL OFFICES AND AGENTS

ADEN. Mitchell Cotts & Co. (Red Sea), Ltd., Cotts House, Crater.

ANGOLA. E. Pinto Basto & Ca., Lda., 1 Avenida 24 de Julho, Lisbon. Sub-Agent: Sociedad Electro-Mecanica Lda., Luanda.

ARGENTINA. Establecimientos Argentinos Marconi, Avenida Cordoba 645, Buenos Aires.

AUSTRALIA. Amalgamated Wireless (Australasia), Ltd., 47, York Street, Sydney, N.S.W.

AUSTRIA. Mr. Wilhelm Pattermann, Rudolfinergasse 18, Vienna XIX.

BARBADOS. The Federal Agency, Knights New Bldg., Bridgetown.

BELGIAN CONGO. Soc. Anonyme International de Télégraphie sans Fil, 7B Avenue Georges Moulaert, Leopoldville.

BELGIUM. Société Belge Radio-Electrique S.A., 66, Chaussée de Ruisbroek, Forest-Bruxelles.

BOLIVIA. MacDonald & Co. (Bolivia) S.A., La Paz.

BRAZIL. Murray Simonsen S.A., Avenida Rio Branco 85, Rio de Janeiro, and Rua Alvares Penteado 208, São Paulo.

BRITISH EAST AFRICA. (Kenya, Uganda, Tanganyika, Zanzibar.) Boustead & Clarke, Ltd., "Mansion House", Nairobi, Kenya.

BRITISH GUIANA. Sprostons Ltd., Lot 4, Lombard Street, Georgetown.

BRITISH WEST AFRICA. (Gambia, Nigeria, Sierra Leone.) Marconi's Wireless Telegraph Co., Ltd., West African Regional Office, 1 Victoria Street, Lagos, Nigeria.

BURMA. Burmese Agencies, Ltd., 245-49, Sule Pagoda Road, Rangoon.

CANADA. Canadian Marconi Co., Marconi Building, 2442, Trenton Avenue, Montreal 16.

CEYLON. Walker Sons & Co., Ltd., Main Street, Fort, Colombo.

CHILE. Gibbs & Cia. S.A.C., Agustinas 1161, Santiago.

COLOMBIA. Riccardi & Cia. Ltda., Calle 13 No. 12-16, Bogota.

COSTA RICA. Distribuidora, S.A., San Jose.

CUBA. Audion Electro Acustica, Calzada 164, Casi Esquina A.L., Vedado-Habana.

CYPRUS. S.A. Petrides & Son, Ltd., 63, Arsinoe Street, Nicosia.

DENMARK. Sophus Berendsen A/S, "Orstedhus", Vester Farimagsgade 41, Copenhagen V.

ECUADOR. Compañia Pan Americana de Comercio S.A., Boulevard 9 de Octubre 620, Guayaquil.

EGYPT. The Pharaonic Engineering & Industrial Co., 33, Sharia Orabi, Cairo.

ERITREA. Mitchell Cotts & Co. (Red Sea) Ltd., Via F. Martini 21-23, Asmara.

ETHIOPIA. Mitchell Cotts & Co. (Red Sea), Ltd., Addis Ababa.

FAROE ISLANDS. S. H. Jakobsen, Radiohandil, Torshavn.

FINLAND. Oy Mercantile A.B., Mannerheimvagen 12, Helsinki.

FRANCE. SIEDMA, 9 Av. de l'Opera, Paris 1.

GERMANY. Kirchfeld KG., Breitestr. 3, Dusseldorf.

GHANA. Marconi's Wireless Telegraph Co. Ltd., Opera Bldg., Pagan St., Accra.

GOA. E. Pinto Basto & Ca., Lda., 1, Avenida 24 de Julho, Lisbon. Sub-Agent: M. S. B. Caculo, Cidade de Goa (Portuguese India).

GREECE. P. C. Lycourezos, Ltd., Kanari Street 5, Athens.

GUATEMALA. Compania Distribuidora Kepaco, S.A. 9A, Avenida No. 20-06, Guatemala, C.A.

HONDURAS. (Republic.) Maquinaria y Accesorios S. de R.L., Tegucigalpa, D.C.

HONG KONG. Marconi (China), Ltd., Queen's Building, Chater Road.

ICELAND. Orka H/F, Reykjavik.

INDIA. Marconi's Wireless Telegraph Co., Ltd., Chawdhary Building, "K" Block, Connaught Circus, New Delhi.

INDONESIA. Yudo & Co., Djalan Pasar Minggu, 1A, Djakarta.

IRAN. Haig C. Galustian & Sons, Shahreza Avenue, Teheran.

IRAQ. Kumait Co., Ltd., Baghdad.

ISRAEL. Middle East Mercantile Corpn., Ltd., 5, Levontin Street, Tel-Aviv.

ITALY. Marconi Italiana S.p.A., Via Corsica No. 21, Genova.

JAMAICA. The Wills Battery Co., Ltd., 2, King Street, Kingston.

JAPAN. Cornes & Co., Ltd., Maruzen Building, Nihonbashi, Tokyo.

KOREA. The International Development Co. (N.Z.) Ltd., 602, Bando Bldg., 1st Street, Ul Chi Ro, Choong Ku, Seoul.

KUWAIT. Gulf Trading & Refrigerating Co., Ltd., Kuwait, Arabia.

LEBANON. Mitchell Cotts & Co. (Middle East), Ltd., Kassatly Building, Rue Fakhry Bey, Beirut.

LIBYA. Mitchell Cotts & Co. (Libya), Ltd., 3, Maidan Asciuhada, Tripoli.

MALTA. Sphinx Trading Co., 57, Fleet Street, Gzira.

MOZAMBIQUE. E. Pinto Basto & Ca., Lda., 1 Avenida 24 de Julho, Lisbon. Sub-Agent: Entreposto Commercial de Mocambique, African Life 3, Avenida Aguiar, Lourenco Marques.

NETHERLANDS. Algemene Nederlandse Radio Unie N.V., Wijnhaven 58, Rotterdam.

NEW ZEALAND. Amalgamated Wireless (Australasia), Ltd., Anvil House, 138 Wakefield Street, Wellington, C.1.

NORWAY. Norsk Marconikompani, 35 Munkedamsveien, Oslo.

PAKISTAN. International Industries, Ltd., 1, West Wharf Road, Karachi.

PANAMA. Cia. Henriquez S.A., Avenida Bolivar No. 7.100, Colon.

PARAGUAY. Acel S.A., Oliva No. 87, Asuncion.

PERU. Milne & Co. S.A., Lima.

PHILIPPINES. Radio Electronic Headquarters Inc., 173 Gomez Street, San Juan, Rizal, Manila.

PORTUGAL AND PORTUGUESE COLONIES. E. Pinto Basto & Ca., Lda., 1, Avenida 24 de Julho, Lisbon.

RHODESIA & NYASALAND. Marconi's Wireless Telegraph Co., Ltd., Central Africa Regional Office, Century House, Baker Avenue, Salisbury.

SALVADOR. As for Guatemala.

SAUDI ARABIA. Mitchell Cotts & Co. (Sharqieh), Ltd., Jedda.

SINGAPORE. Marconi's Wireless Telegraph Co., Ltd., Far East Regional Office, 35, Robinson Road, Singapore.

SOMALILAND PROTECTORATE. Mitchell Cotts & Co. (Red Sea), Ltd., Street No. 8, Berbera.

SOUTH AFRICA. Marconi (South Africa), Ltd., 321-4, Union Corporation Building, Marshall Street, Johannesburg.

SPAIN AND SPANISH COLONIES. Marconi Española S.A., Alcala 45, Madrid.

SUDAN. Mitchell Cotts & Co. (Middle East), Ltd., Victoria Avenue, Khartoum.

SWEDEN. Svenska Radioaktiebolaget, Alstromergatan 12, Stockholm.

SWITZERLAND. Hasler S.A., Belpstrasse, Berne.

SYRIA. Levant Trading Co., 15-17, Barada Avenue, Damascus.

THAILAND. Yip in Tsoi & Co., Ltd., Bangkok.

TRINIDAD. Masons & Co., Ltd., Port-of-Spain.

TURKEY. G. & A. Baker, Ltd., Prevuayans Han, Tahtakale, Istanbul, and S. Soyal Han, Kat 2 Yenisehir Ankara.

URUGUAY. Regusci & Voulminot, Avenida General Rondeau 2027, Montevideo.

U.S.A. Mr. J. S. V. Walton, 23-25 Beaver Street, New York City 4, N.Y.

VENEZUELA. English Electric de Venezuela C.A., Edificio Pan American, Avda. Urdaneta, Caracas.

YUGOSLAVIA. Standard, Terazije 39, Belgrade.